T_C's higher than the one of Nb for the RF

A Super-Superconductor

Enzo Palmieri

Legnaro National Laboratories
ISTITUTO NAZIONALE di FISICA NUCLEARE
and
Padua University – Material Science Departement, ITALY

Argonne National Laboratories,IL, Sept 21 2004

At a given angular frequency **ω**, the surface impedance $\mathbf{Z_n}$ for a normal metal, in the normal regime, can be written as

$$Z_n = \frac{1 - i}{\sigma_n \delta} = (1 - i)\frac{\rho_n}{\delta}$$

where $\boldsymbol{\sigma_n = 1 / \rho_n}$ is the dc conductivity at the working temperature;
δ is the skin depth

Extension to Superconductors:

$\sigma_1 - i\,\sigma_2$ in place of σ_n

As derived by Nam, for T < Tc / 2

R_s can be approximated by

$$\frac{R_s}{R_n} = \frac{1}{\sqrt{2}} \frac{\sigma_1 / \sigma_n}{\left(\sigma_2 / \sigma_n\right)^{3/2}}$$

In the framework of the BCS theory extension at finite frequencies, Mattis and Bardeen found, for $\omega < 2\Delta$, the two following integral relations for the complex conductivity of a superconductor:

$$\frac{\sigma_1}{\sigma_n} = \frac{2}{h'\omega}\int_{\Delta}^{\infty}\left(f(E) - f(E + h'\omega)\right) g^{+}(E)\, dE$$

$$\frac{\sigma_2}{\sigma_n} = \frac{1}{h'\omega}\int_{\Delta - h'\omega,\ -\Delta}^{\Delta}\left(1 - 2 f(E + h'\omega)\right) g^{-}(E)\, dE$$

$$2\Delta = s\ K T_C,$$

$$f(E) = \frac{1}{\left(1 + e^{E/KT}\right)}$$

$$g^{\pm}(E) = \frac{E^2 + \Delta^2 + h'\omega E}{\left(\pm(E^2 - \Delta^2)\right)^{1/2}\left((E + h'\omega)^2 - \Delta^2\right)^{1/2}}$$

The two integrals σ1/σn and σ2/σn are easily numerically calculated.

In the normal skin effect regime, for $h'\omega \ll 2\Delta$

they can be approximated by two analytical expressions:

$$\frac{\sigma_1}{\sigma_n} = \left[\frac{2\Delta/KT}{\left(1 + e^{-\Delta/KT}\right)^2} \right] e^{-\Delta/KT} \ln \frac{\Delta}{h'\omega}$$

$$\frac{\sigma_2}{\sigma_n} = \frac{\pi\Delta}{h'\omega} \tanh \frac{\Delta}{2KT}$$

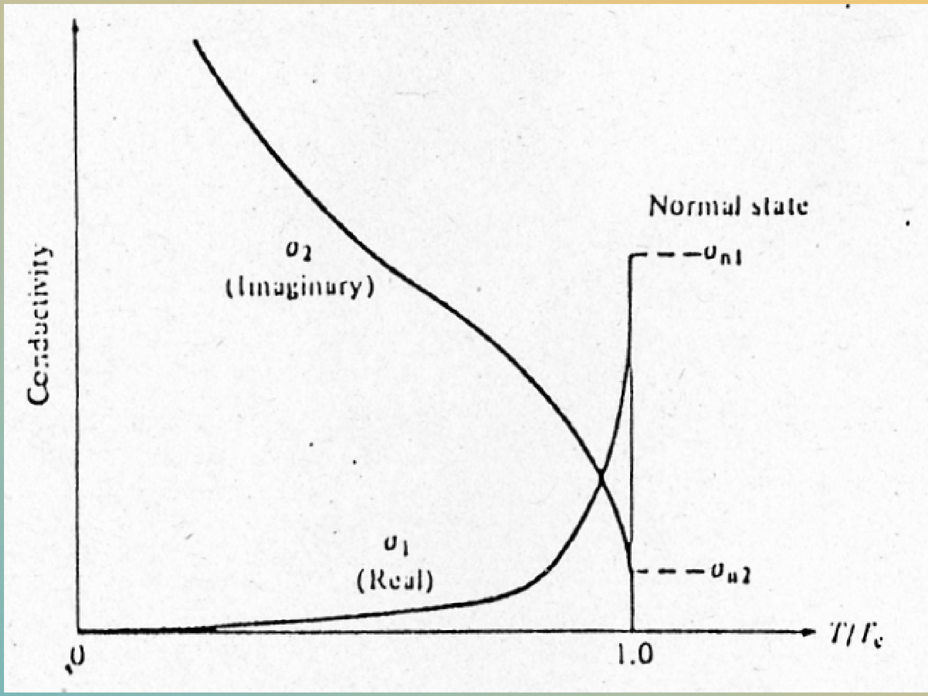

Then, if T < Tc / 2

$$R_{BCS} \cong \frac{R_n}{\sqrt{2}}\left(\frac{h'\omega}{\pi\Delta}\right)^{3/2}\frac{\sigma_1}{\sigma_n} = A\rho_n^{1/2}\frac{e^{-\frac{\Delta}{KT_C}}}{\sqrt{sT_c}\,T\left(1+e^{-\frac{\Delta}{KT_c}}\right)^2}\,\omega^2 \ln\frac{\Delta}{h'\omega}$$

with $A = 6 \cdot 10^{-21} \left[\frac{\Omega K^3}{m\,s^4}\right]^{1/2}$

For low rf losses, a high T_C value it is not sufficient

A metallic behaviour is mandatory

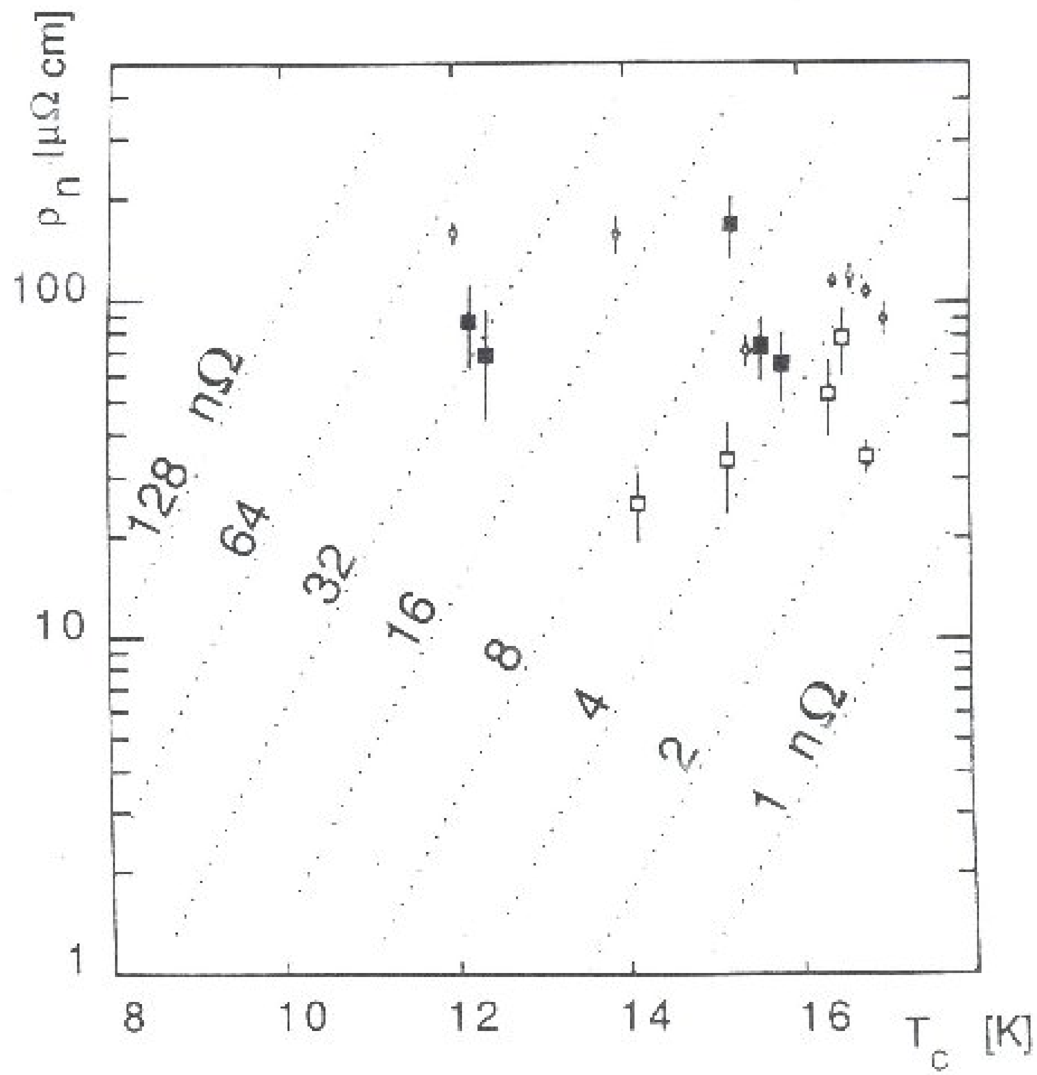

Fig. 1 Lines of equal R_{BCS} at 4.2 K and 500 MHz in the bidimentional space (ρ_n, T_c). Fixed the working temperature (T = 4.2 K), and the frequency (f = 500 MHz), R_{BCS} depends only on the energy gap and on the normal state resistivity. The Tc scale is draft for the case s = 4. For comparison Nb coated cavities provide R_{BCS} = 55 nΩ. The experimental data refer to: sputtered films of (NbTi)N at 200 C (full square); (NbTi)N at 600 C (empty square); NbN at 200 C

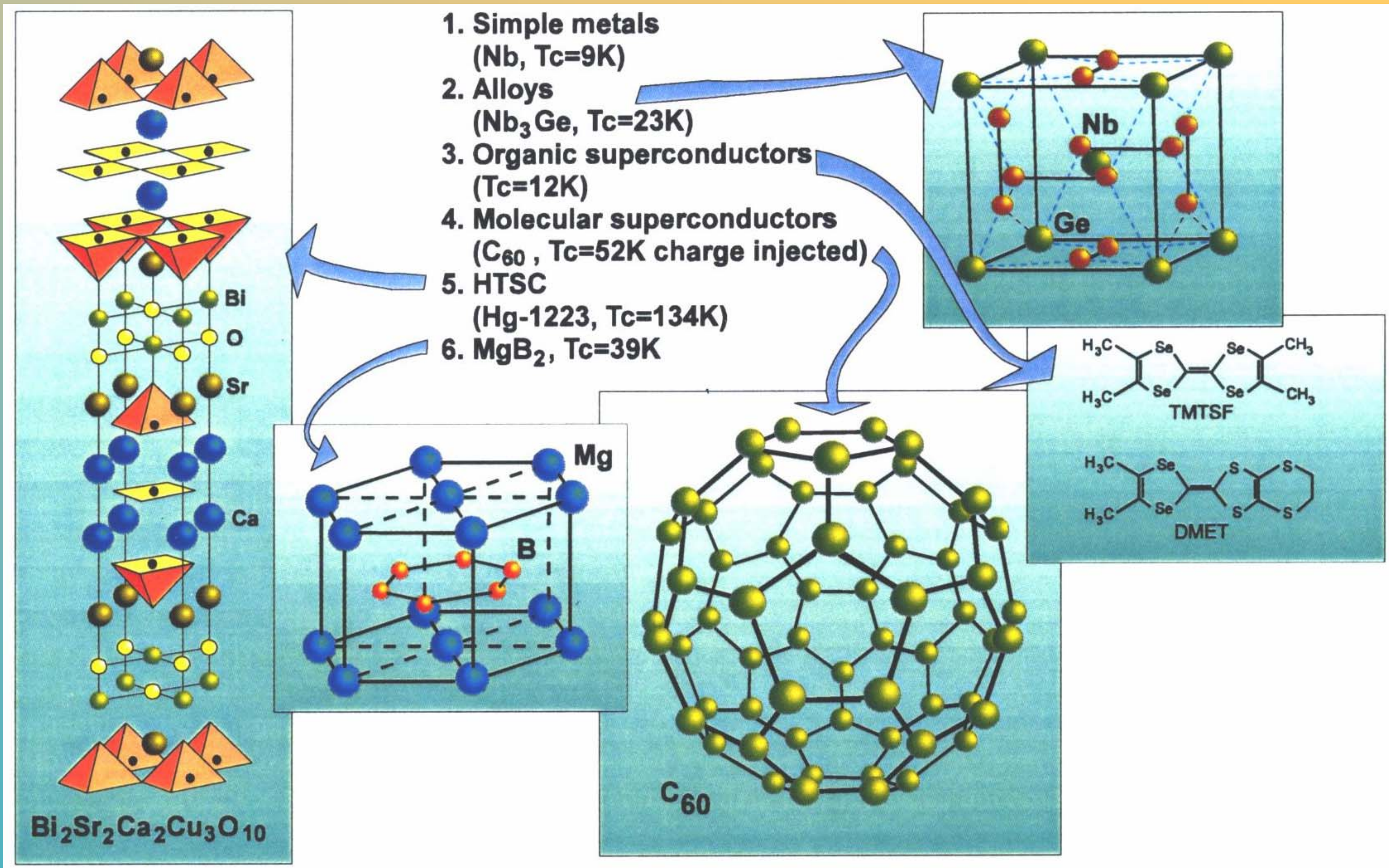

Different classes of superconductors (after Buzea and Yamashita).

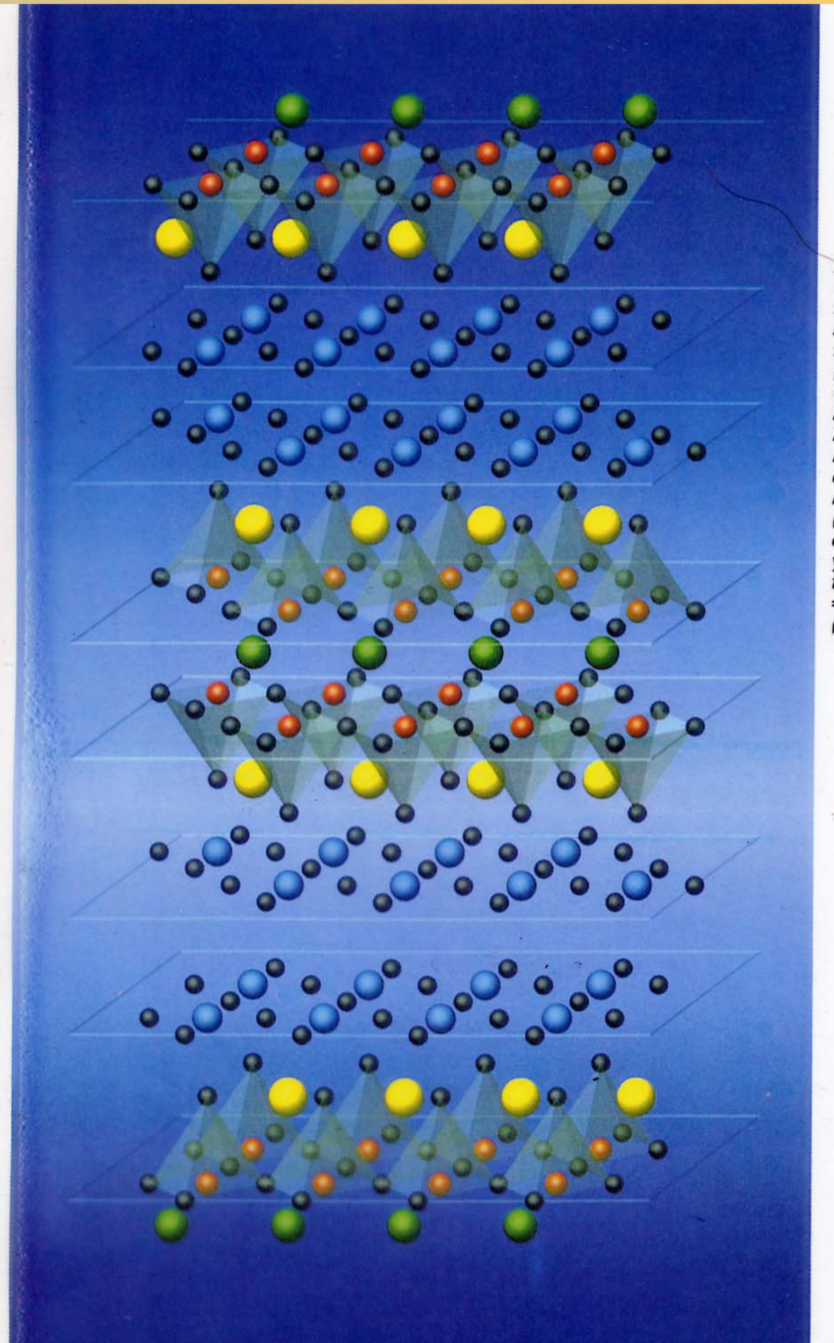

Fig. 1
Crystal structure of the superconductor type $Bi_2(Sr_{1-y}Ca_y)_3Cu_2O_{10-\delta}$ developed by Hoechst.
Key: green = calcium (Ca), red = copper (Cu), black = oxygen (O), yellow = strontium (Sr), blue = bismuth (Bi).

Mat. Res. Soc. Symp. Proc. Vol. EXS-3 © 2004 Materials Research Society EE9.9.1

PERCOLATION, SURFACE IMPEDANCE and PINNING in MgB_2-, and HTS-SUPERCONDUCTORS.

J. Halbritter, Forschungszentrum Karlsruhe
Institut für Materialforschung
Postfach 36 40
76021 Karlsruhe

ABSTRACT

The hindrance of electric transport by grain/island boundary resistances R_{bn} (Ωcm^2) in distances a_J ($\lesssim 1\mu m$) is well accepted in the normal conducting transport in granular materials. In contrast, in superconducting transport such boundaries enhance by the related critical Josephson current density j_{cJ} the critical current density by Josephson fluxons (JF). For a quantitative model the resistivity

$$\rho(T) = R_{bn}/a_J + p\,(\rho^i\,(T) + \rho^i\,(0))$$

is fitted to observations with percolation factors $p > 1$ by current diverting boundaries with $R_{bn} \gtrsim m\Omega cm^2$. HTS show $p > 1 - 10$, critical current densities $j_c(H< H_{C1}) \simeq j_{cJ}(H)$ by JF pinning with $j_{cJ}R_{bn} \approx 10^{-12}\ V\Omega m^2/R_{bn} << \Delta/e$, rf residual losses $R_{res} \propto \omega^2/a_J\, j_{cJ}^{3/2}\, R_{bn}$ and hysteresis losses $R_{hys} \propto \omega H/a_J\, j_{cJ}$. In MgB_2 films percolation with $p \gtrsim 2 - 50$, with $j_c(H < H_{c1}) \simeq j_{cJ}(H)$ and $j_{cJ}\, R_{bn} \approx \Delta/e$ is found. Whereas percolation decreases conductivities via the boundary resistances R_{bn} in the normal state always, pinning of JF enhances $j_c(H<H_{c1}) \simeq j_{cJ}(H)$ dominated in dc transport by chains of strongest links. In contrast, rf surface impedances via $R_{res}\,(T,\omega) \propto \omega^2/j_{cJ}(T)^{3/2}$ and $R_{hys}\,(T,H) \propto \omega H/j_{cJ}(T)$ are dominated by the weakest links and deteriorate by weak links always. But in all cases where $\rho(T)$ deviates from Matthiessen law, RRR values are not sufficient to describe material quality, but a proper percolation analysis is needed to forcast via $R_{bn} \propto j_{cJ}^{-n}$ ($n \simeq 1$ -2) superconducting properties below H_{c1} in dc and rf.

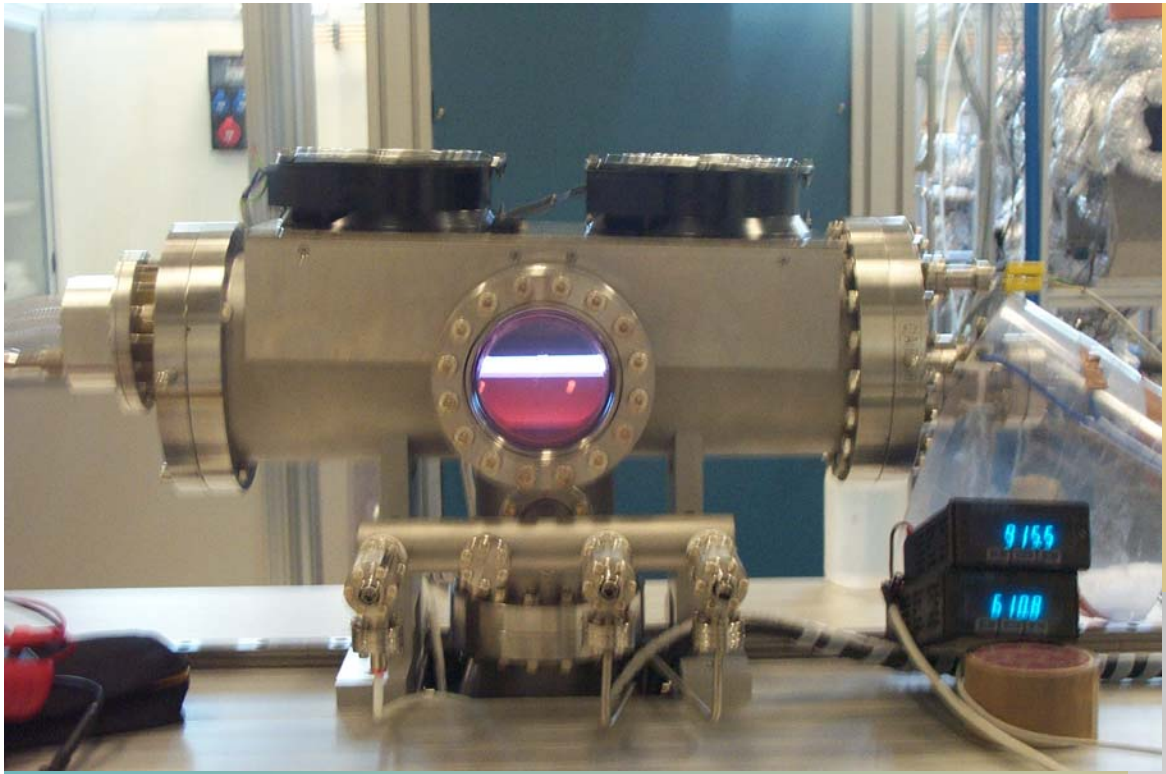

YBCO thin films on large area substrates

P.Romano, A. Vecchione,
G. Keppel and V. Palmieri

DIODE Sputtering at **950 C at 1 mbar**

onto sapphire, and SrTiO3

Distance cathode substrate = 10 mm

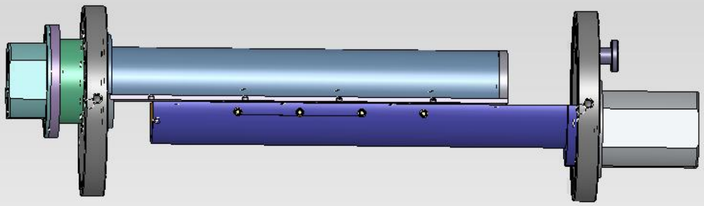

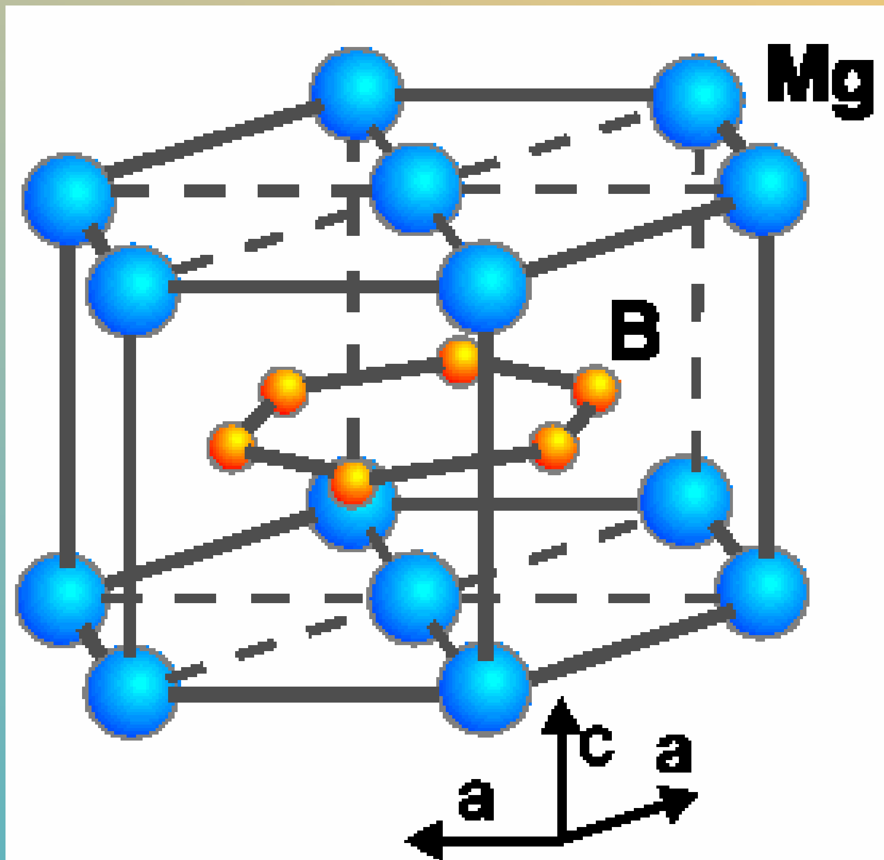

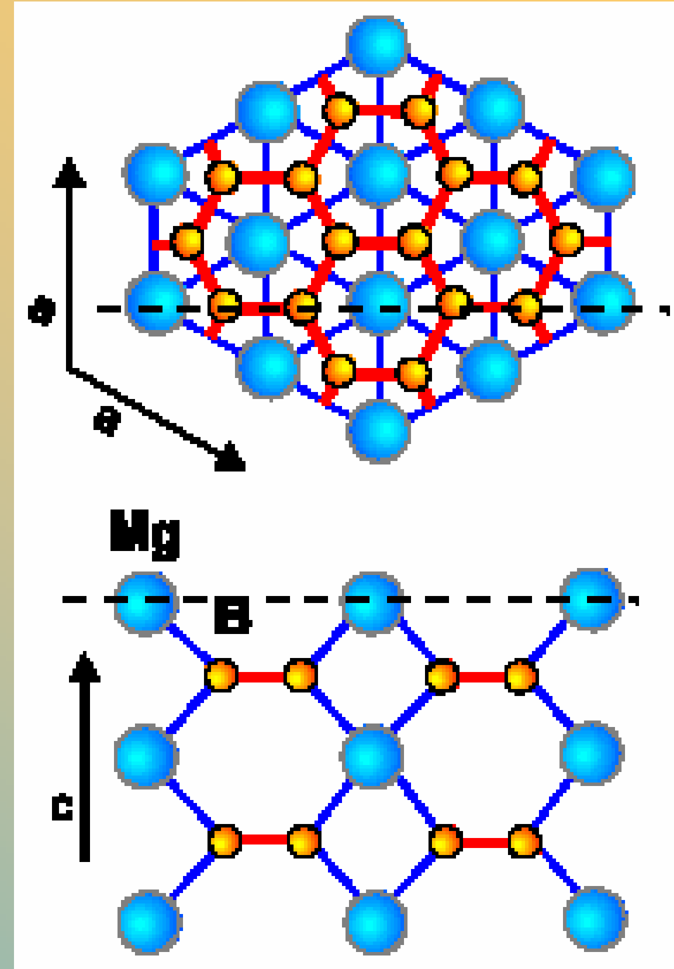

Structure of MgB_2 containing graphite-type B layers separated by hexagonal close-packed layers of Mg

(After Buzea and Yamashita)

And what about the problem of film degradataion due to water exposure???

Activity on MgB2 at Los Alamos Neutron Science Center

Report by **Tsuyoshi Tajima**

Bulk samples by HIP

- No degradation with high-pressure water rinse
- Surface polishing with 0.1mm diamond lapping paper reduced Rs significantly

Giorgio Keppel, Thesis 2004,
Material Science Dept, Padua University

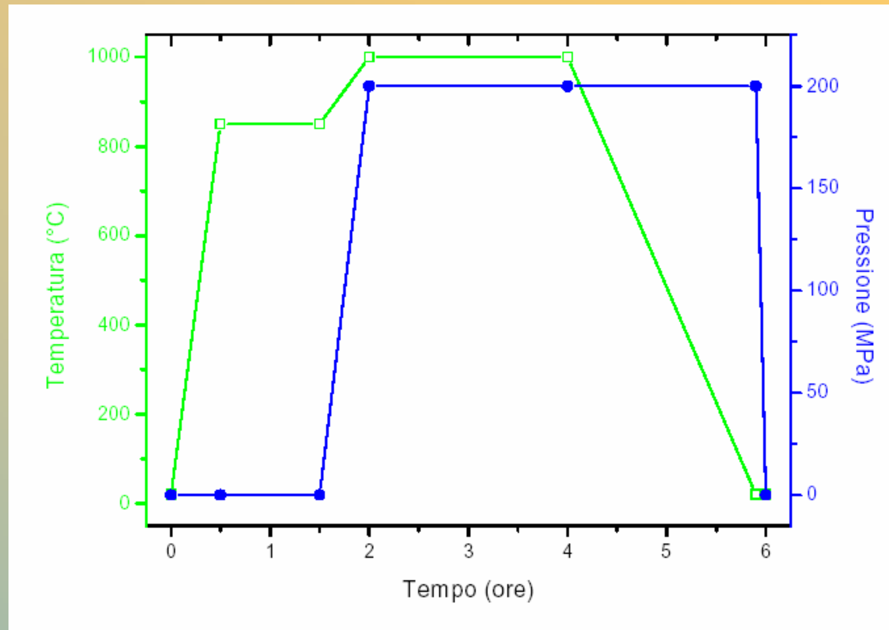

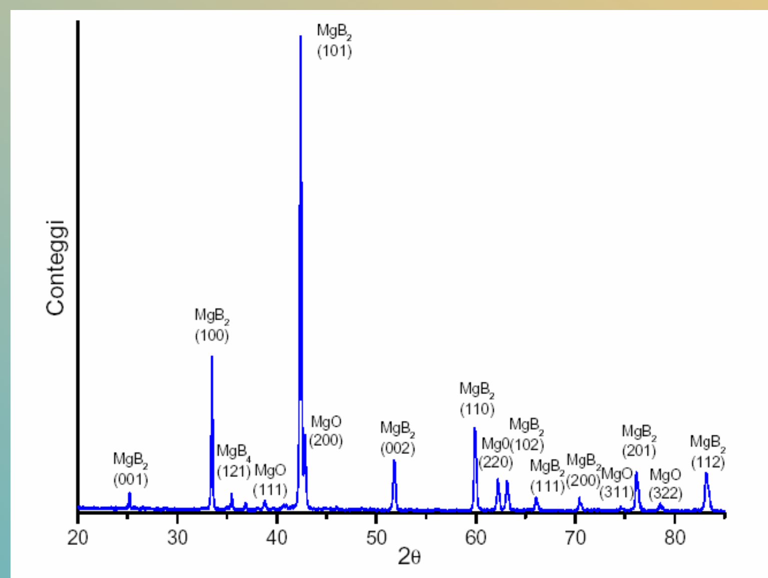

DC Magnetron Sputtering of MgB_2 + Mg

R. Vaglio et al. Naples University

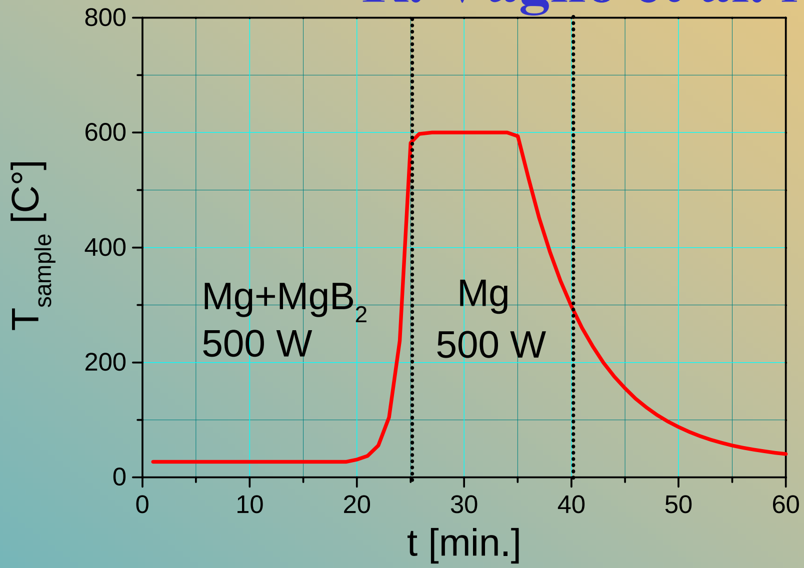

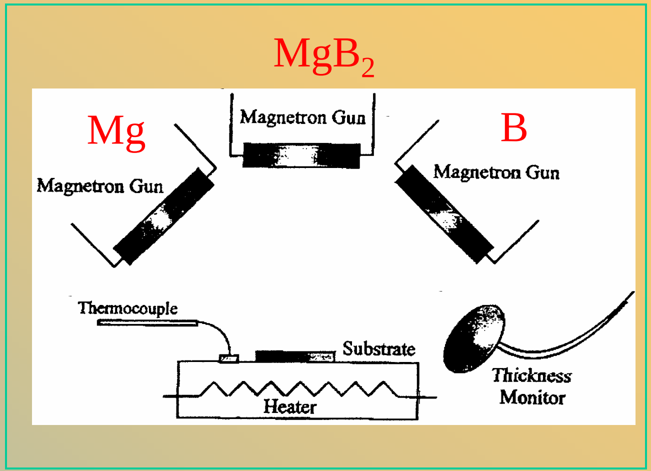

Films are deposited by an in-situ process in two steps:

DC Magnetron Sputtering of MgB_2 and Mg targets at room temperature

Post-annealing at increasing temperature (300°C - 600°C) in Mg sputtering

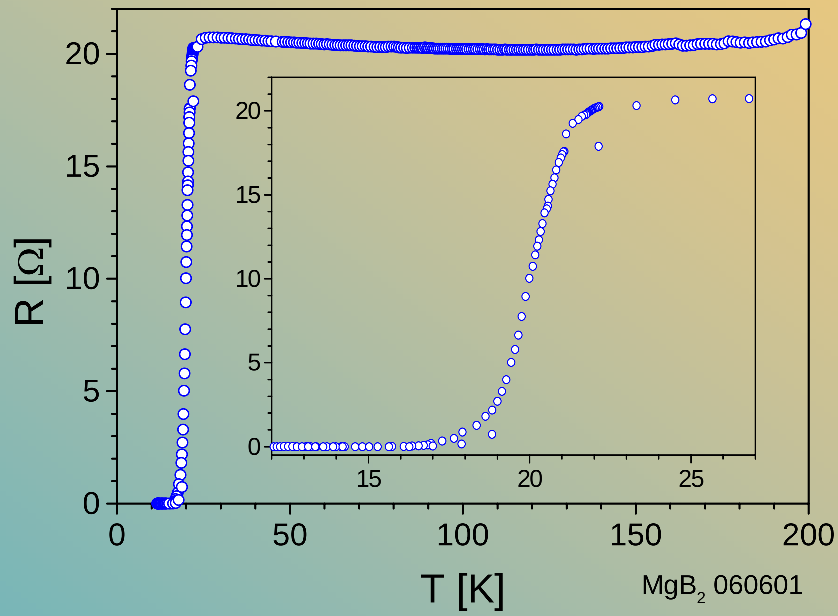

DC Pulsed Sputtering of MgB_2 + Mg Powders

V. Palmieri, A. Calore, I.I. Kulik

Advantages: The added Mg compensates the lost one. Targets are self-made. One can immediately prepare targets out of stoichiometry or with the addition of other elements.
Disadvantages: Possible leaking of Magnesium during the sputtering process.

Room temperature substrate

Substrate Temperature = 500 C

No Postannealing

T-dependence of the order parameter from fit with the one-gap model.Δ_{dirty}(T) and Δ_{3D}(T) from fit with the two-gap model. Fit to BCS curves

T-dependence of the order parameter from fit with the one-gap model.Δ_{dirty}(T) and Δ_{3D}(T) from fit with the two-gap model. Fit to BCS curves

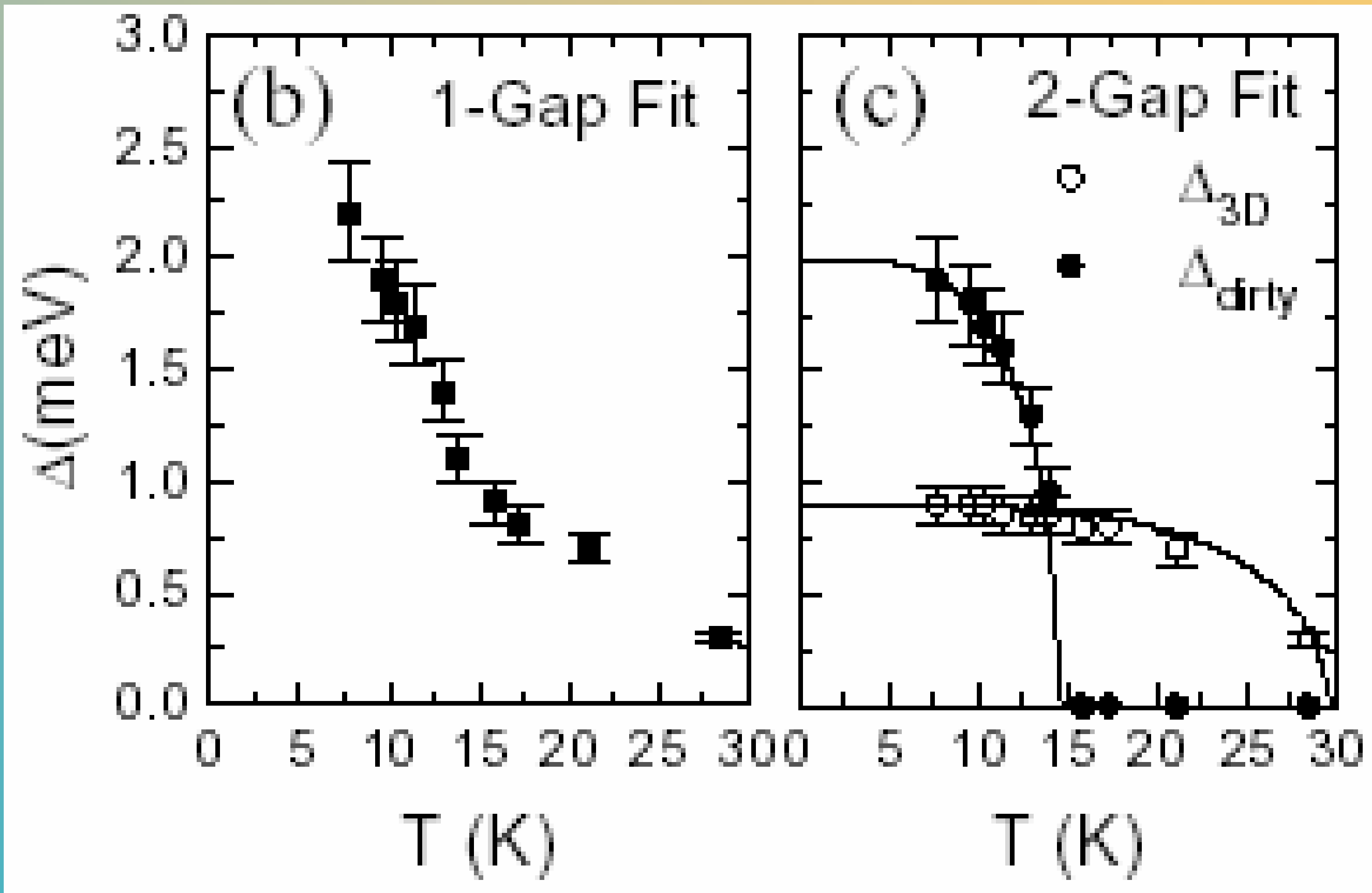

(after G. Carapella, N. Martucciello, G. Costabile, C. Ferdeghini, V. Ferrando, and G. Grassano)

Gap parameters

from specific heat and spectroscopic experiments:

Technique	$2\Delta_1(0)/k_B T_c$	$2\Delta_2(0)/k_B T_c$	$\gamma_1 : \gamma_2$
specific heat	3.8	1.3	0.5:0.5
specific heat	3.9	1.3	0.5:0.5
specific heat	4.4	1.2	0.55:0.45
penetration depth	4.6	1.6	0.60:0.40
tunneling	4.5	1.9	
Raman	3.7	1.6	
point-contact	4.1	1.7	
photoemission	3.6	1.1	
band structure	4	1.3	0.53:0.47

(After A. Junod, Y. Wang, .F. Bouquet, P. Toulemonde)

Two fluid model

Three fluid model

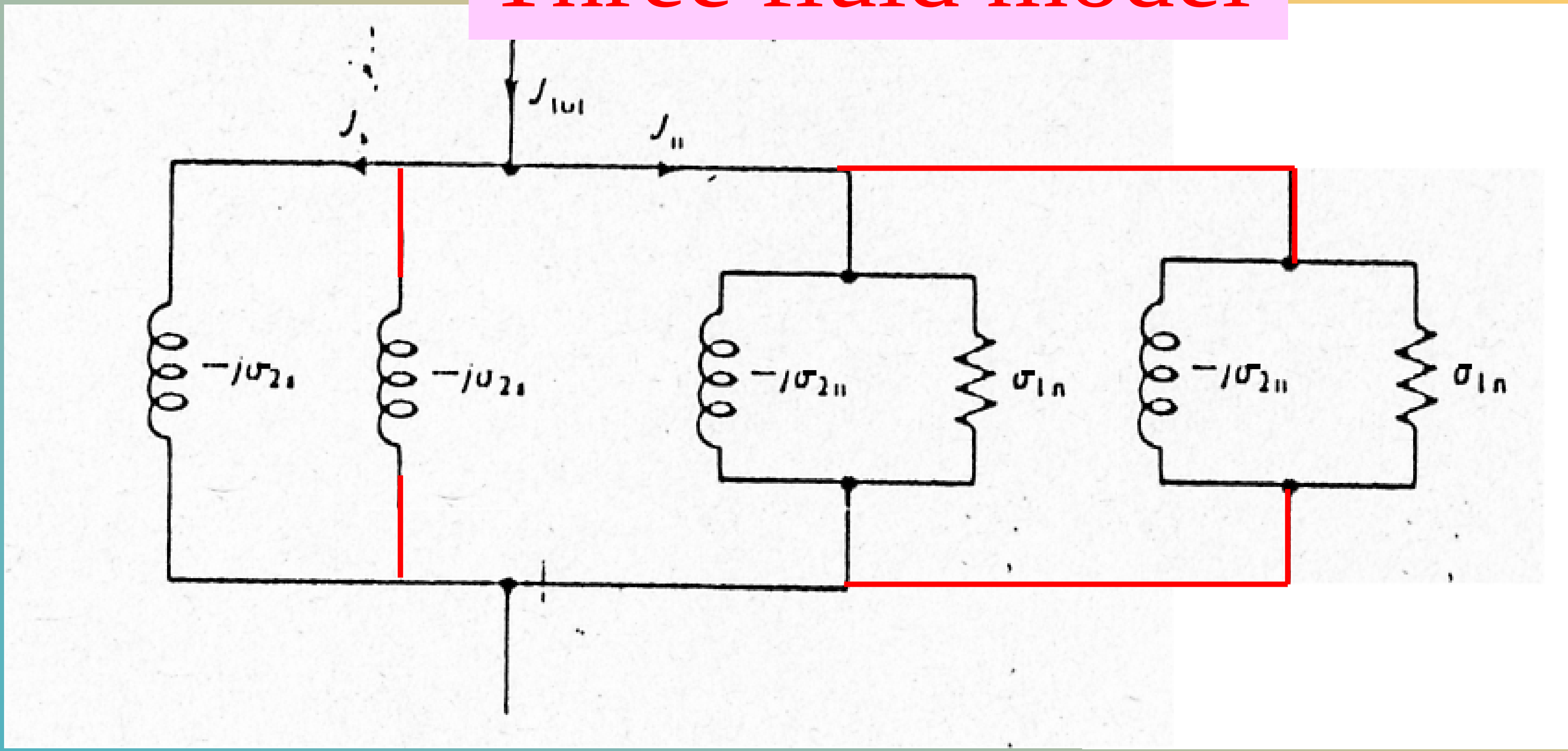

Equivalent circuit for the admittance of a unit cube of superconductor

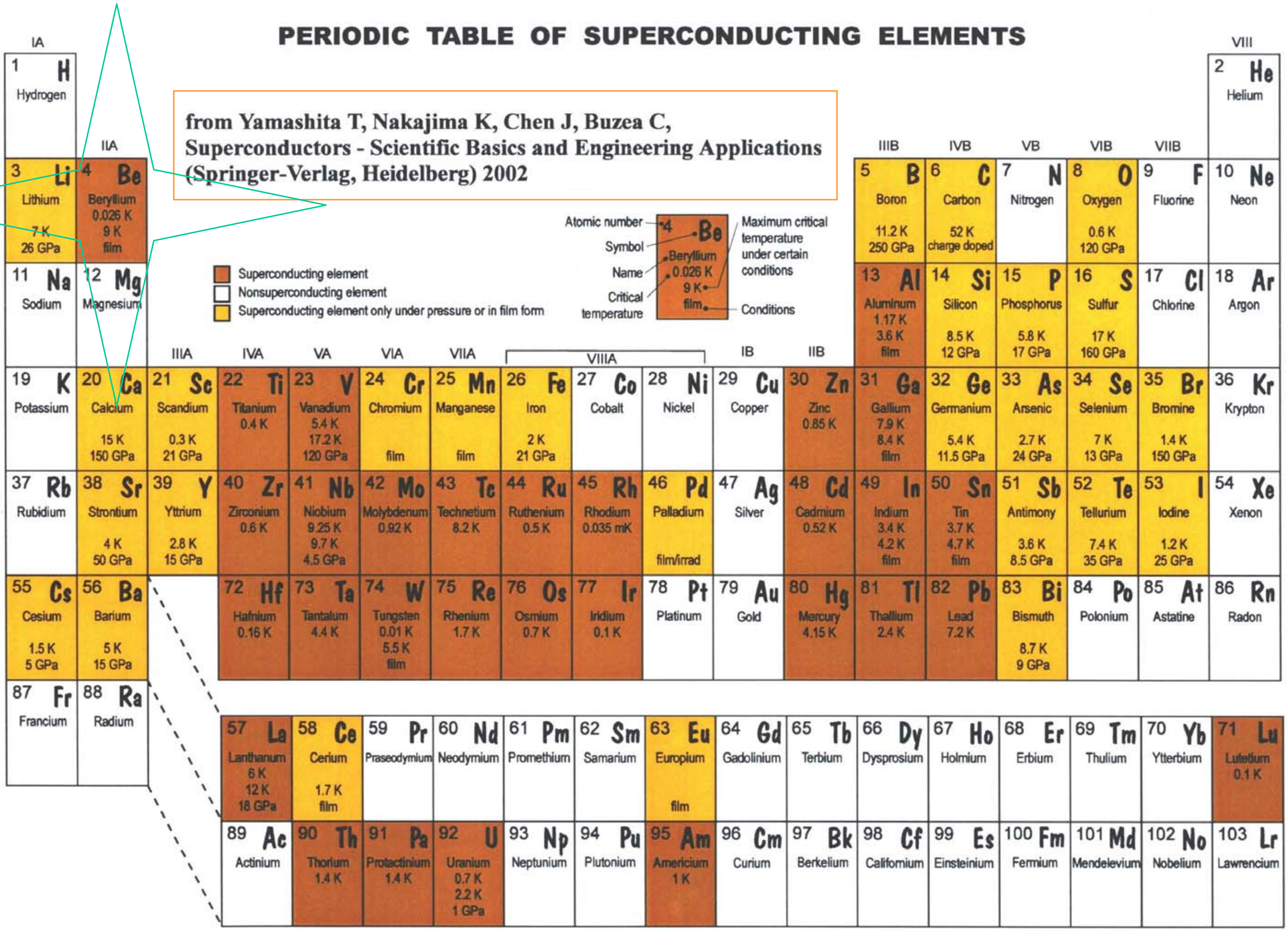

Figure 4. Periodic Table of elements with critical temperature at normal pressure, and maximum critical temperature attained under certain conditions (pressure, film form or charge injected) [Yamashita].

In the **Tl-Pb-Bi** System, the mass can be held almost constant and the variation of $\mathbf{T_C}$ with **e/a** can be studied in a continuous fashion even up to **9 K**

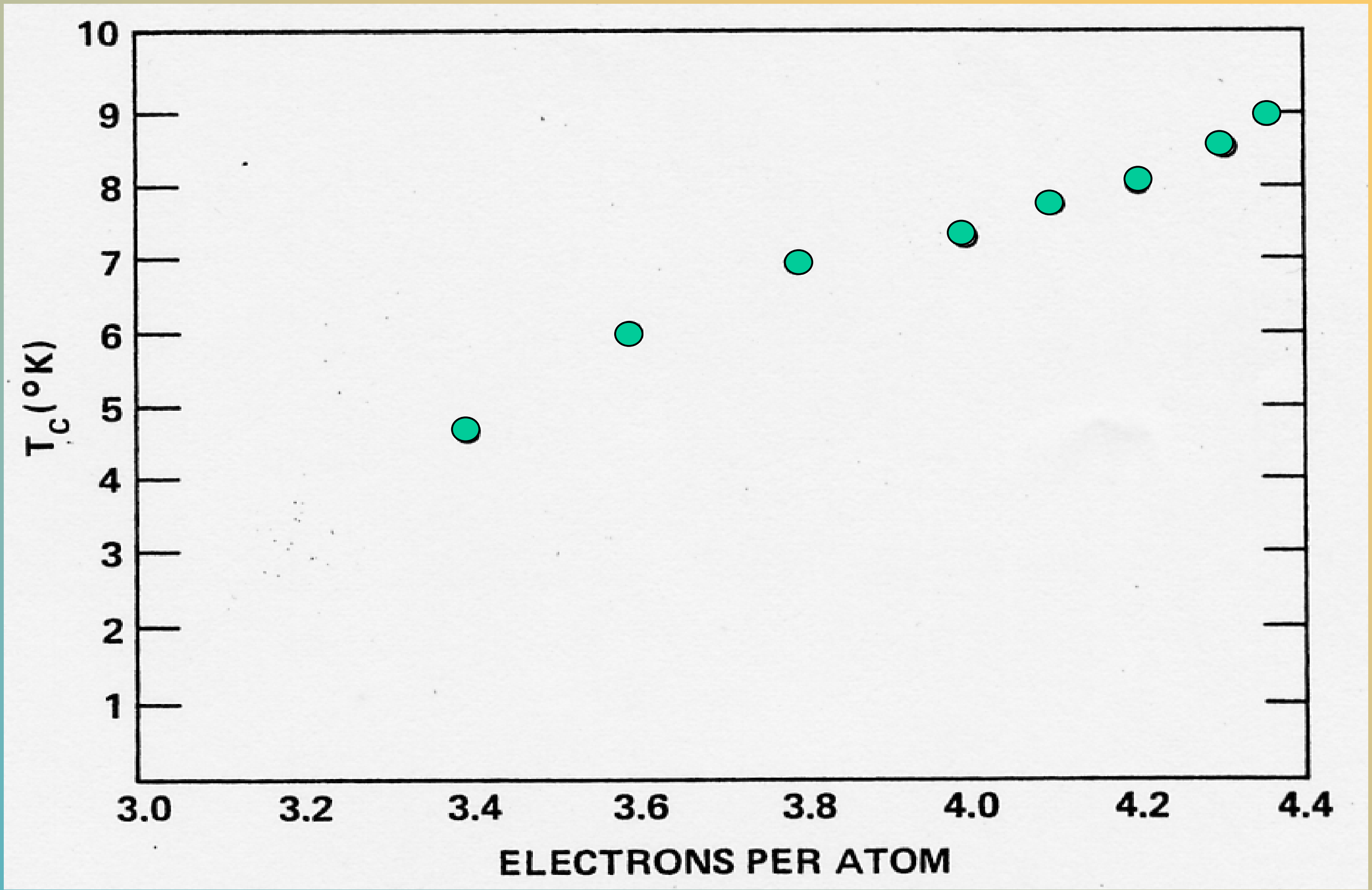

Variation of Transition Temperature with electrons-to-atom ratio in the Tl-Pb-Bi alloy family.

After Dynes and Rowell, Phys. Rev. B 11,1884 (1975)

PdH is a very famous material for the reversal isotope effect and it has low resistivity

And Hydrides of Pd-Ag and Pd-Cu display Tc up to 15K!!!

Critical Temperature of compounds with NaCl structure

B \ A	Sc	Y	La	Ti	Zr	Hf	V	Nb	Ta	Cr	Mo	W	Re
B					3.4	3.1							
C	<1.38	<1.38		3.42	<0.3	<1.20	0.03 3.2*	12	10.35		14.3	10.0	3.4
N	<1.38	<1.4	1.35	5.49	10.7	8.83	8.5	17.3	6.5	<1.28	5.0	<1.38	
P			<1.68										
Sb		<1.02	<1.02										
O				2.0			<0.3	1.39					
S	<0.33	1.9	0.87		3.3								
Se	<0.33	2.5	1.02										
Te		2.05	1.48										

* $T_C = 3.2$ K was registered in vanadium carbide after implantation of C^+ ions s

Critical temperature vs composition for nitride and carbide ***addition to NbN***

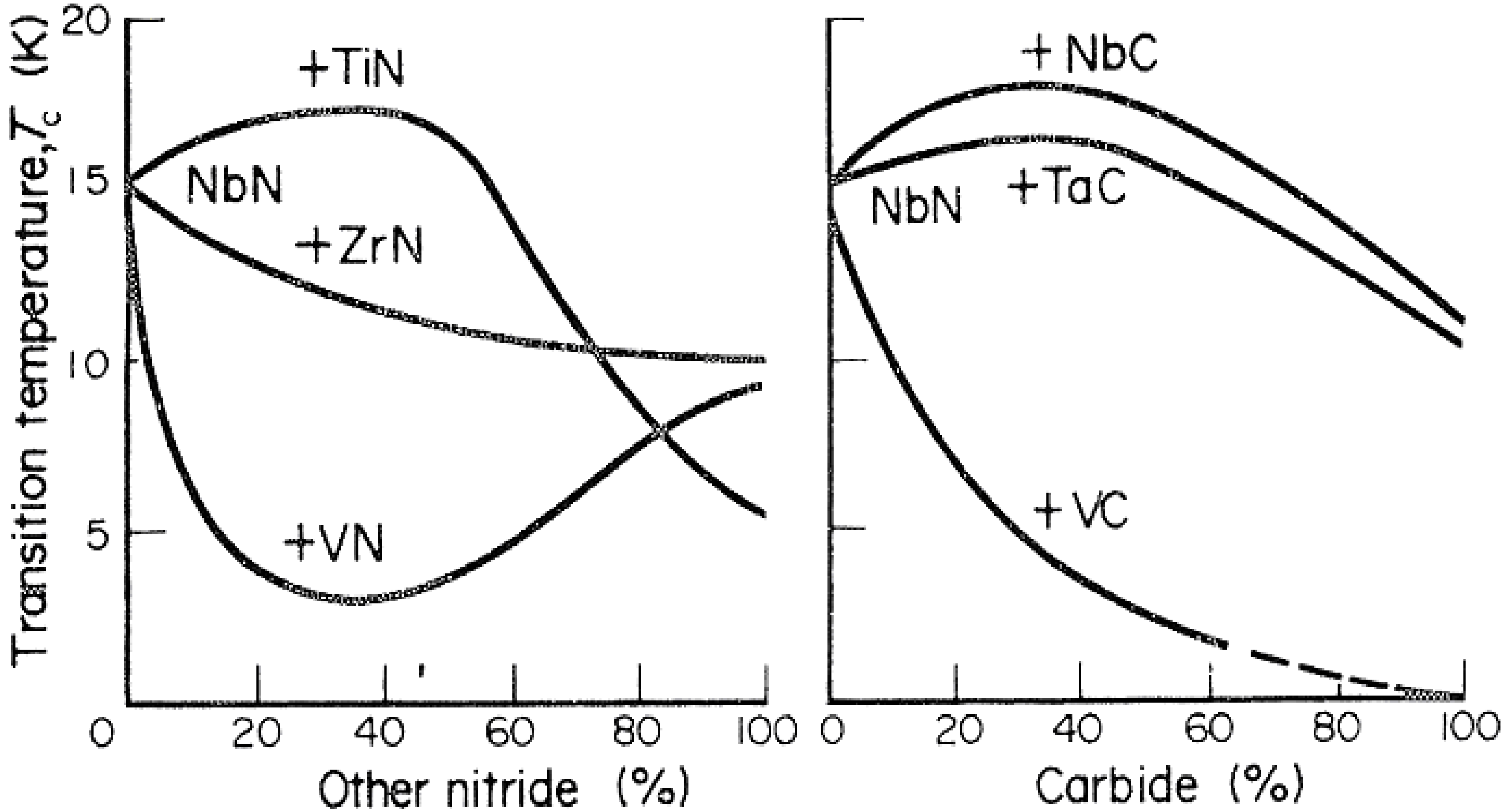

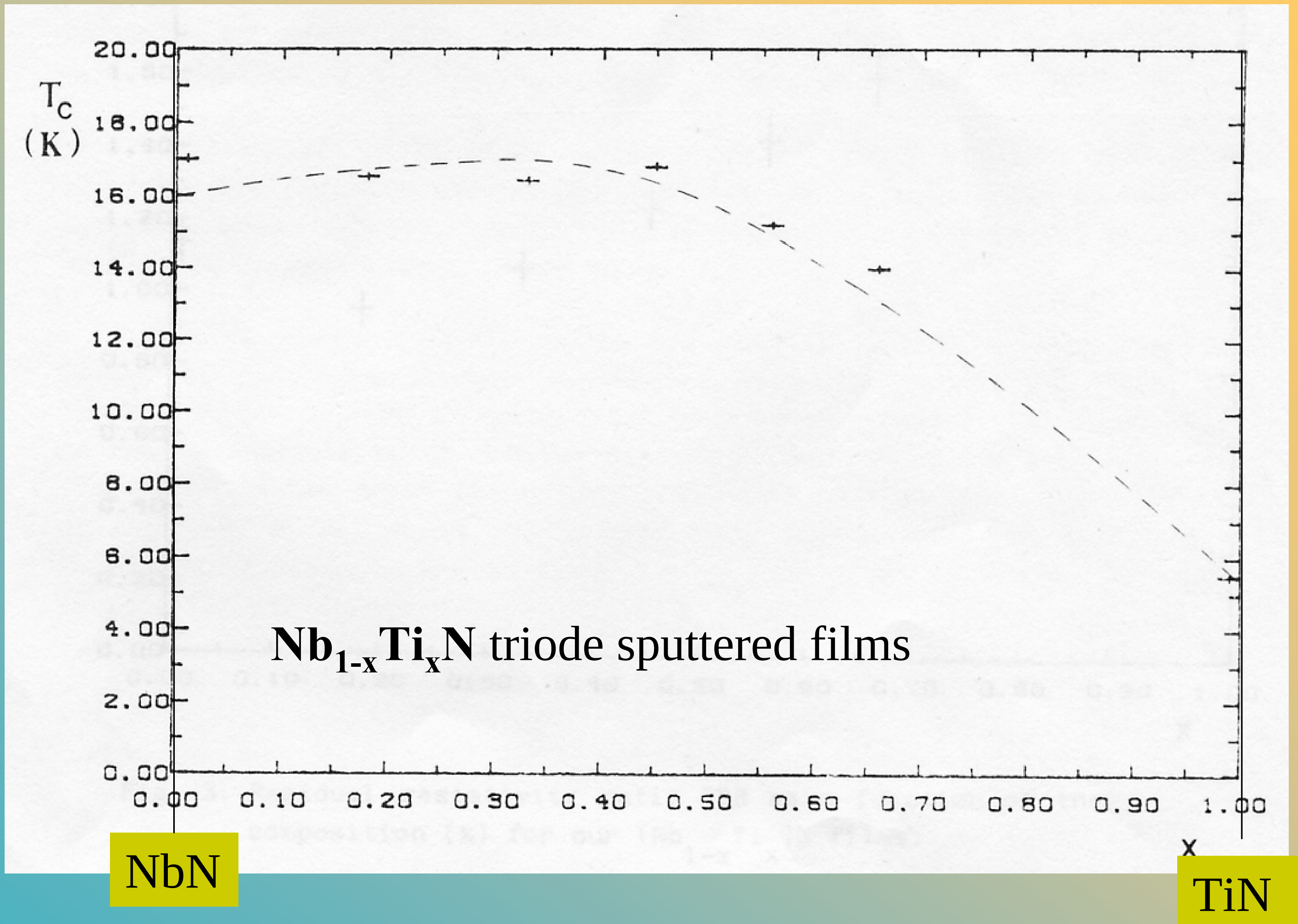

A.Nigro, G.Nobile, V.Palmieri, R.Vaglio, "PROPERTIES OF NIOBIUM-TITANIUM NITRIDE SUPERCONDUCTING THIN FILMS", **Adv. Cryog. Eng. Mat., vol. 34, (1988) 813**

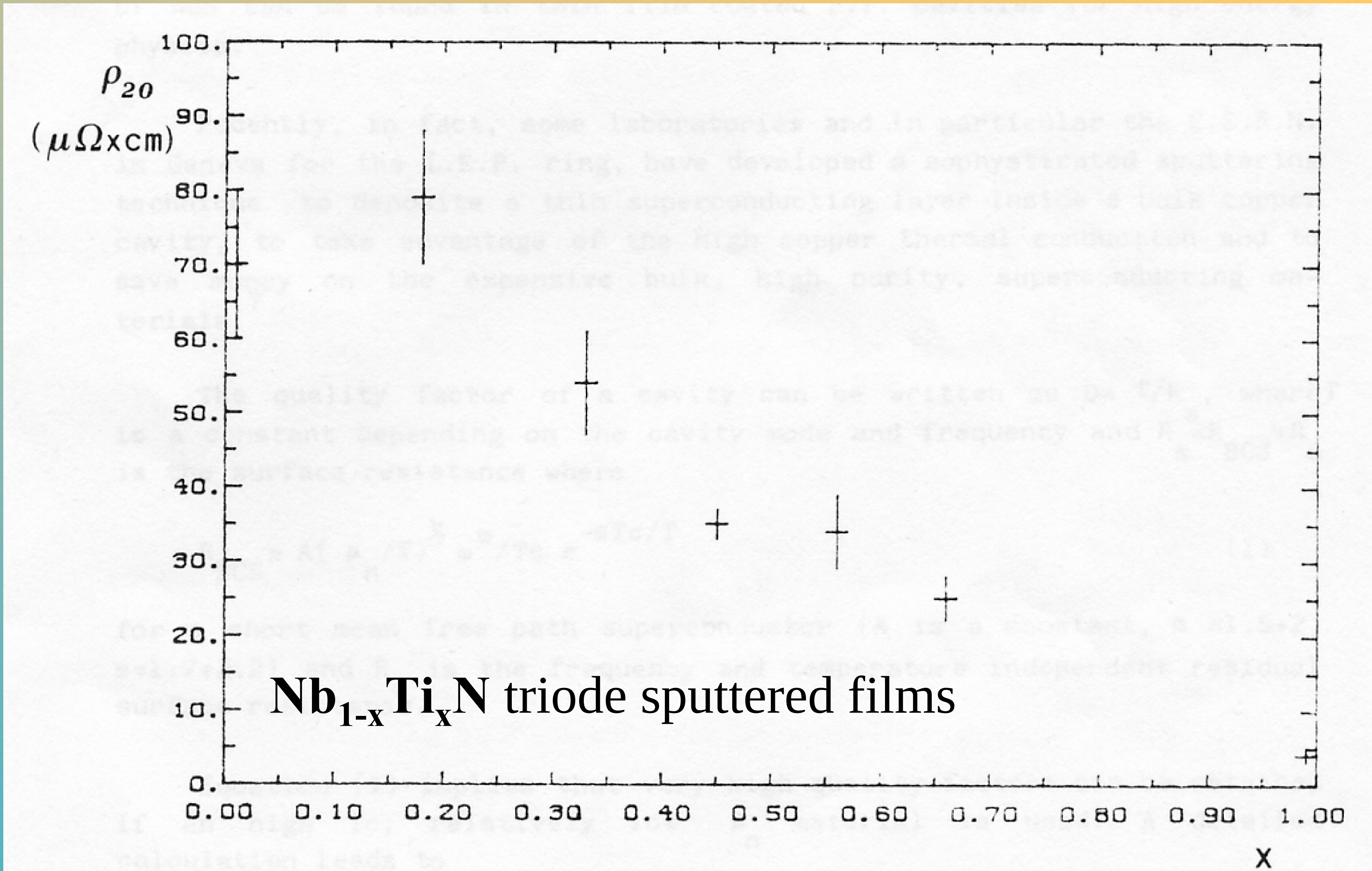

$Nb_{1-x}Ti_xN$ triode sputtered films

NbN

TiN

A.Nigro, G.Nobile, V.Palmieri, R.Vaglio, "PROPERTIES OF NIOBIUM-TITANIUM NITRIDE SUPERCONDUCTING THIN FILMS", **Adv. Cryog. Eng. Mat., vol. 34, (1988) 813**

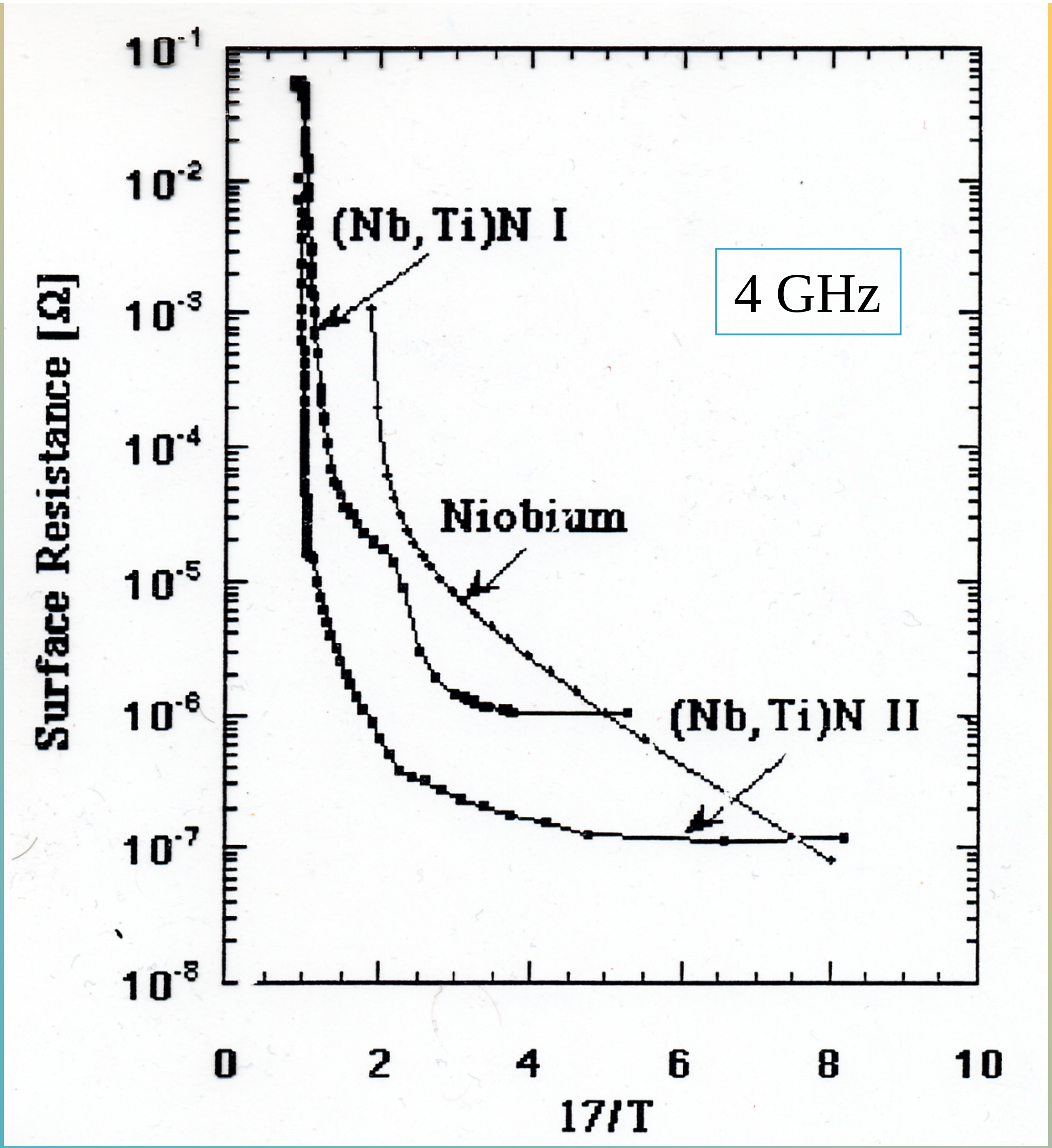

4 GHz
(Nb,Ti)N I
Niobium
(Nb,Ti)N II
Surface Resistance [Ω]
17/T
10-1
10-2
10-3
10-4
10-5
10-6
10-7
10-8
0
2
4
6
8
10

Surface resistance of a $(Nb_{0.55}Ti_{0.45})N/Cu$ film (*4 GHz*)

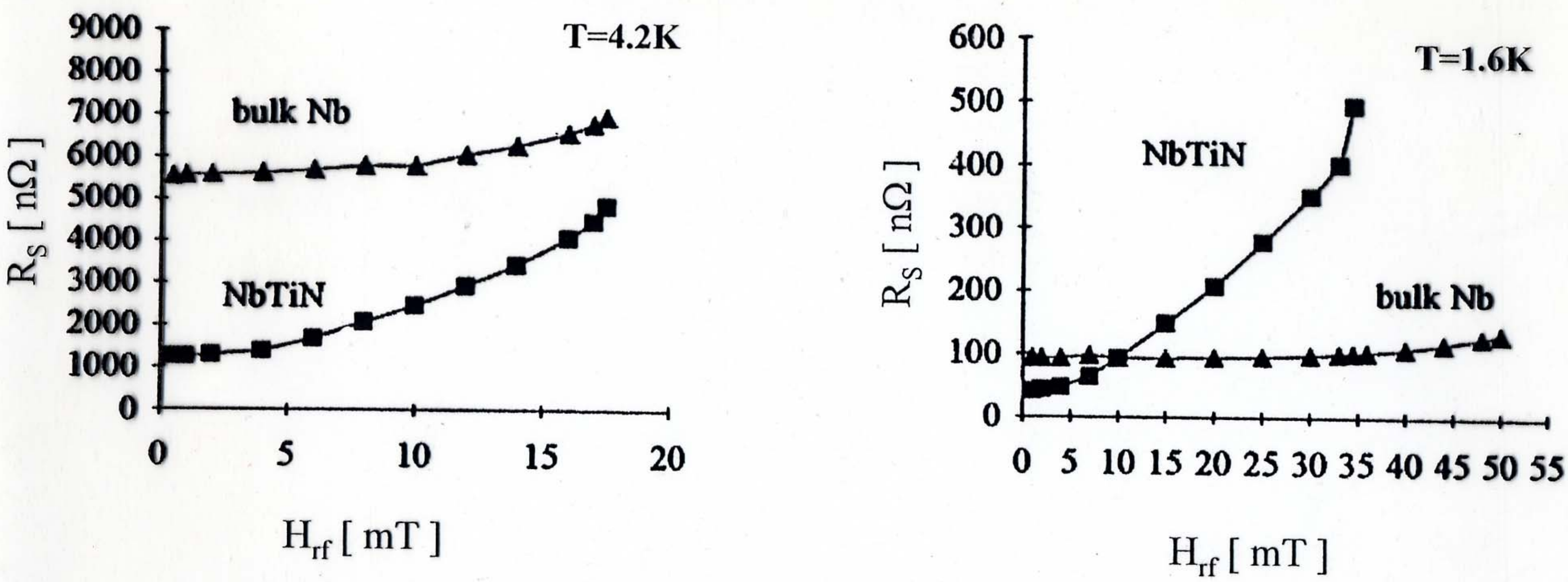

After R. Vaglio et al.

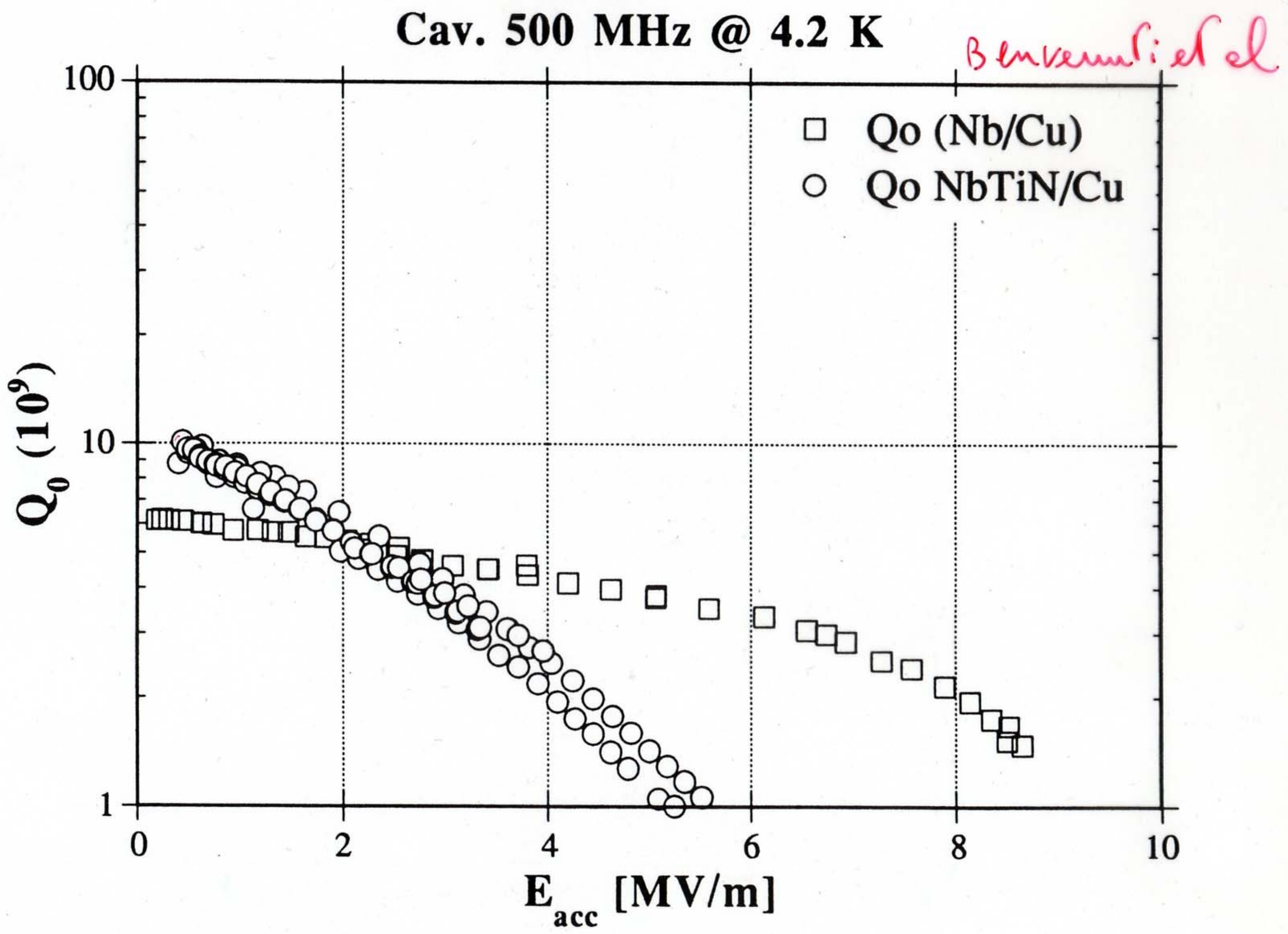

Cav. 500 MHz @ 4.2 K
Benvenuti et al
100
10
1
Q0 (10^9)
Qo (Nb/Cu)
Qo NbTiN/Cu
0
2
4
6
8
10
Eacc [MV/m]

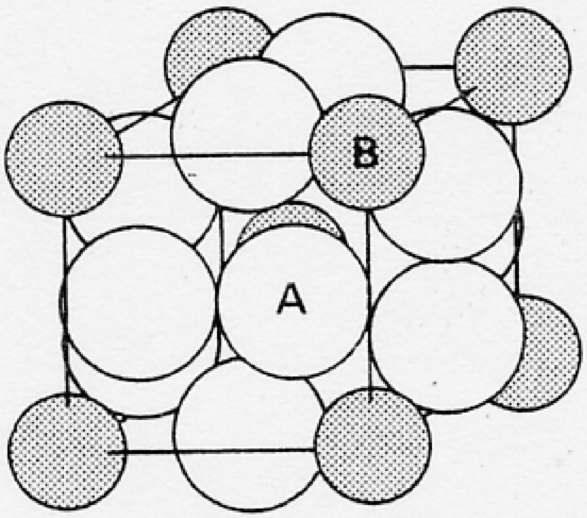

A-15 (OR β-W)
A_3B

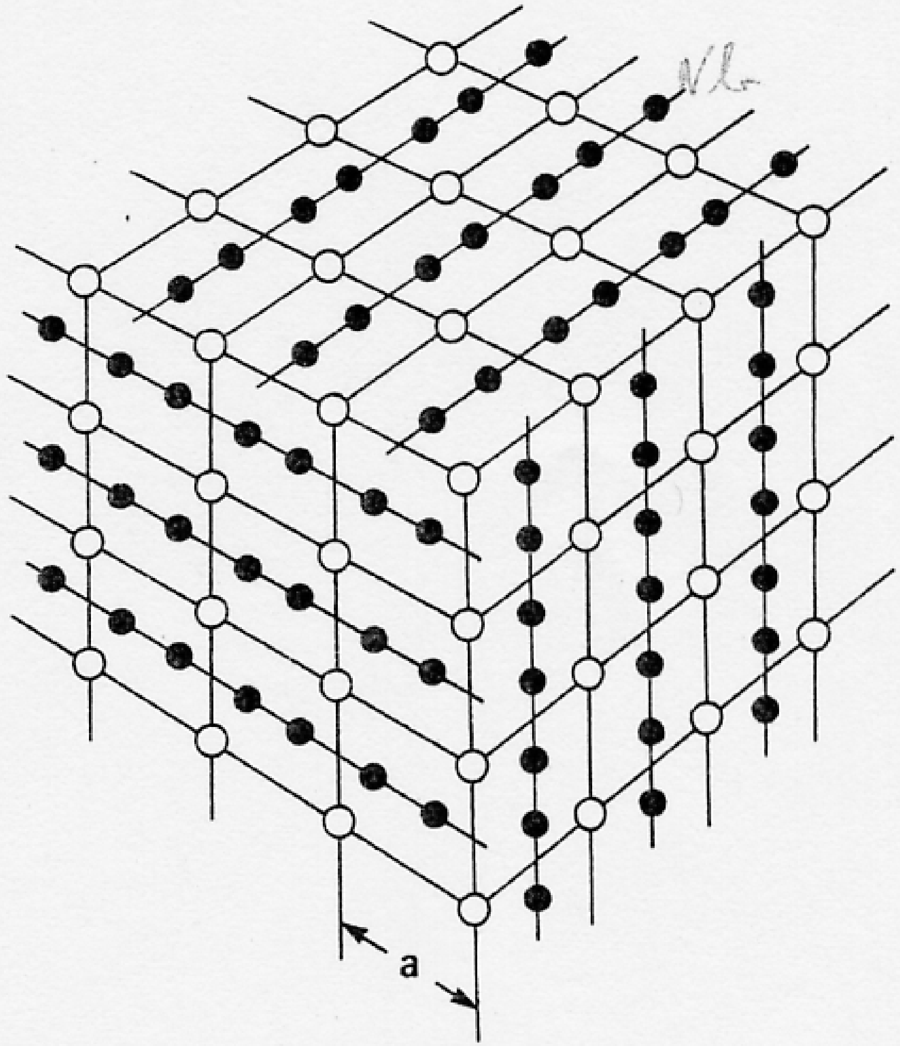

Nontransition elements	T_c (K)	Transition elements	T_c (K)
Ti_3Sb	6.5	Ti_3Ir	4.2
$Zr_{80}Sn_{20}$[a]	0.92	Ti_3Pt	0.5
Zr–Pb	0.76	Zr_3Au	0.9
$Zr_{\sim 3}Bi$[b]	3.4	$V_{29}Re_{71}$	8.4
V–Al[c]	14	$V_{50}Os_{50}$	5.7
V_3Ga	15.9	$V_{65}Rh_{35}$	$\simeq 1$
V_3Si	17.0	$V_{63}Ir_{37}$	1.7
$V_{\sim 3}Ge$	6	$V_{\sim 3}Pd$	0.08
$V_{\sim 3}Ge$[c]	11	V_3Pt	3.7
$V_{\sim 79}Sn_{\sim 21}$	3.8	$V_{76}Au_{24}$	3
$V_{77}As_{23}$	0.2	$Nb_{75}Os_{25}$	1.0
$V_{76}Sb_{24}$	0.8	$Nb_{75}Rh_{25}$	2.6
Nb_3Al	19.1	$Nb_{72}Ir_{28}$	3.2
Nb_3Ga	20.7	Nb_3Pt	11
$Nb_{\sim 3}In$[b]	9.2	$Nb_{\sim 3}Au$	11.5
$Nb_{82}Si_{18}$[a]	4.4	$Ta_{85}Pt_{15}$	0.4
Nb–Si[c]	11–17	$Ta_{\sim 80}Au_{20}$	0.55
Nb–Ge[a]	17	$Cr_{72}Ru_{28}$	3.4
Nb–Ge[c]	23	$Cr_{73}Os_{27}$	4.7
Nb_3Sn	18	$Cr_{78}Rh_{22}$	0.07
Nb–Sb	2	$Cr_{82}Ir_{18}$	0.75
$Nb_{\sim 3}Bi$[b]	3	$Mo_{40}Tc_{60}$	13.4
$Ta_{\sim 3}Ge$[c]	8	$Mo_{\sim 65}Re_{\sim 35}$[c]	$\simeq 15$
$Ta_{\sim 3}Sn$	8.3	$Mo_{75}Os_{25}$	13.1
$Ta_{\sim 3}Sb$	0.7	$Mo_{78}Ir_{22}$	8.5
Mo_3Al	0.58	$Mo_{82}Pt_{18}$	4.6
Mo_3Ga	0.76	$W_{\sim 60}Re_{\sim 40}$[c]	11
$Mo_{77}Si_{23}$	1.7		
$Mo_{77}Ge_{23}$	1.8		

a Rapid quenching b High-pressure synthesis c Film deposition techniques

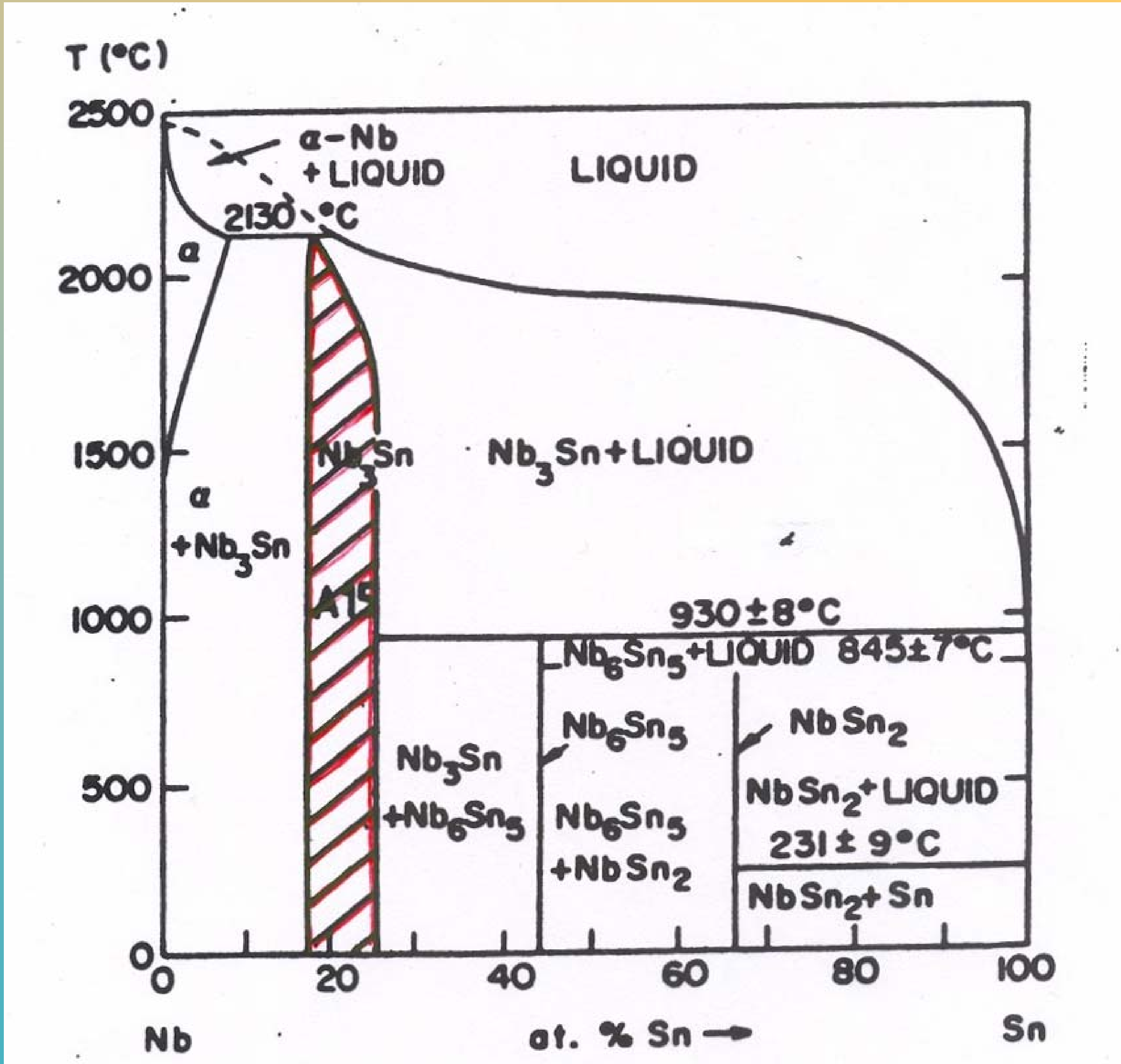

T (°C)
2500
2000
1500
1000
500
0
α-Nb
+ LIQUID
LIQUID
2130 °C
α
α
+Nb3Sn
Nb3Sn
A15
Nb3Sn + LIQUID
930±8°C
Nb6Sn5+LIQUID
845±7°C
Nb6Sn5
NbSn2
Nb3Sn
+Nb6Sn5
Nb6Sn5
+NbSn2
NbSn2+ LIQUID
231 ± 9°C
NbSn2+ Sn
0
20
40
60
80
100
Nb
at. % Sn →
Sn

Nb_3Sn 1.5GHz cavity made at Wuppertal by Sn vapour phase diffusion

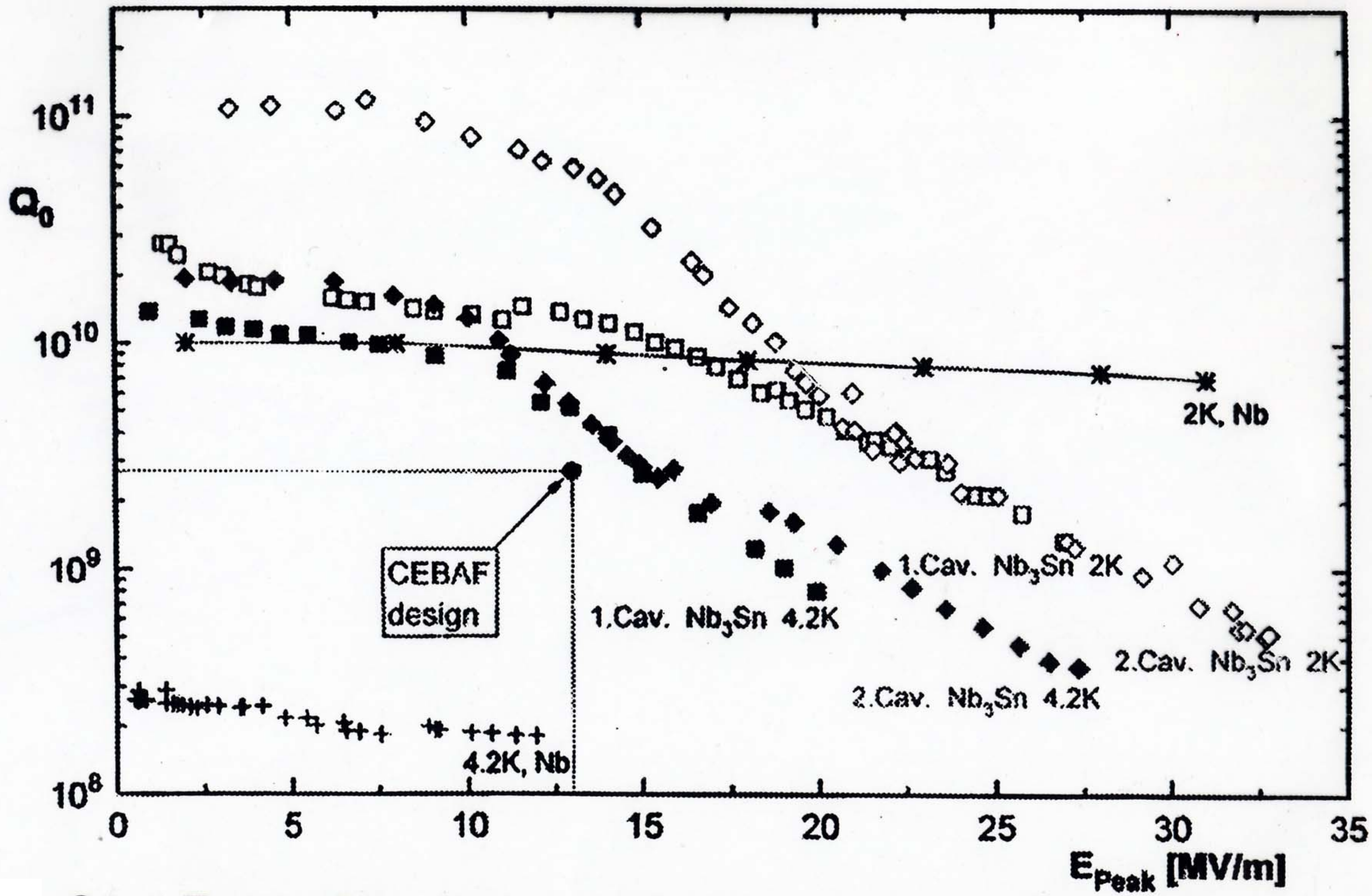

Q vs. Epeak of the first two Nb3SN-coated 1.5 GHz single-cell cavites in comparison to pure Nb at 4.2 K and 2 K from CEBAF.

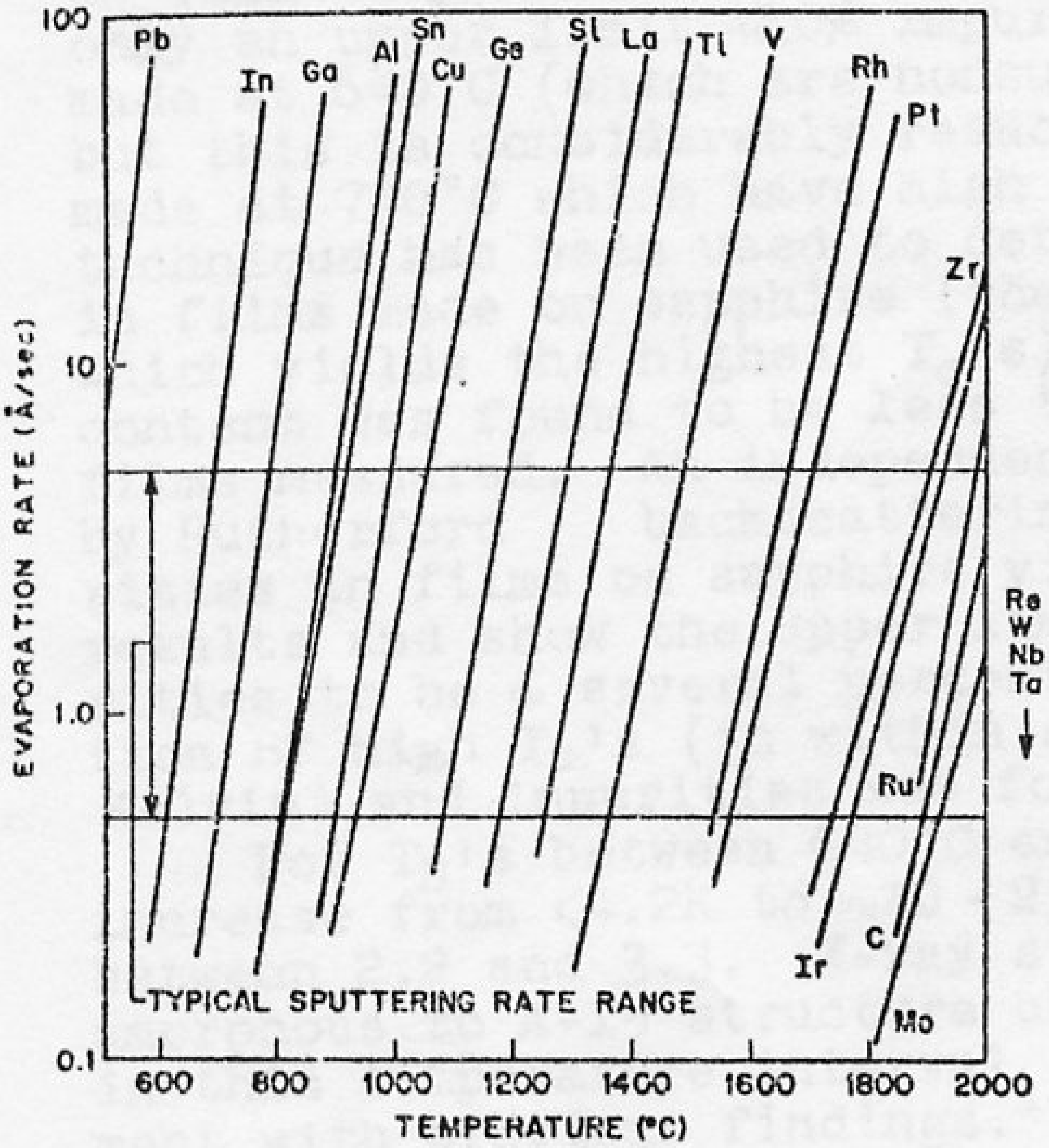

EVAPORATION RATE (Å/sec)
100
10
1.0
0.1
TEMPERATURE (°C)
600
800
1000
1200
1400
1600
1800
2000
Pb
In
Ga
Al
Sn
Cu
Ge
Si
La
Ti
V
Rh
Pt
Zr
Re
W
Nb
Ta
Ru
C
Ir
Mo
TYPICAL SPUTTERING RATE RANGE

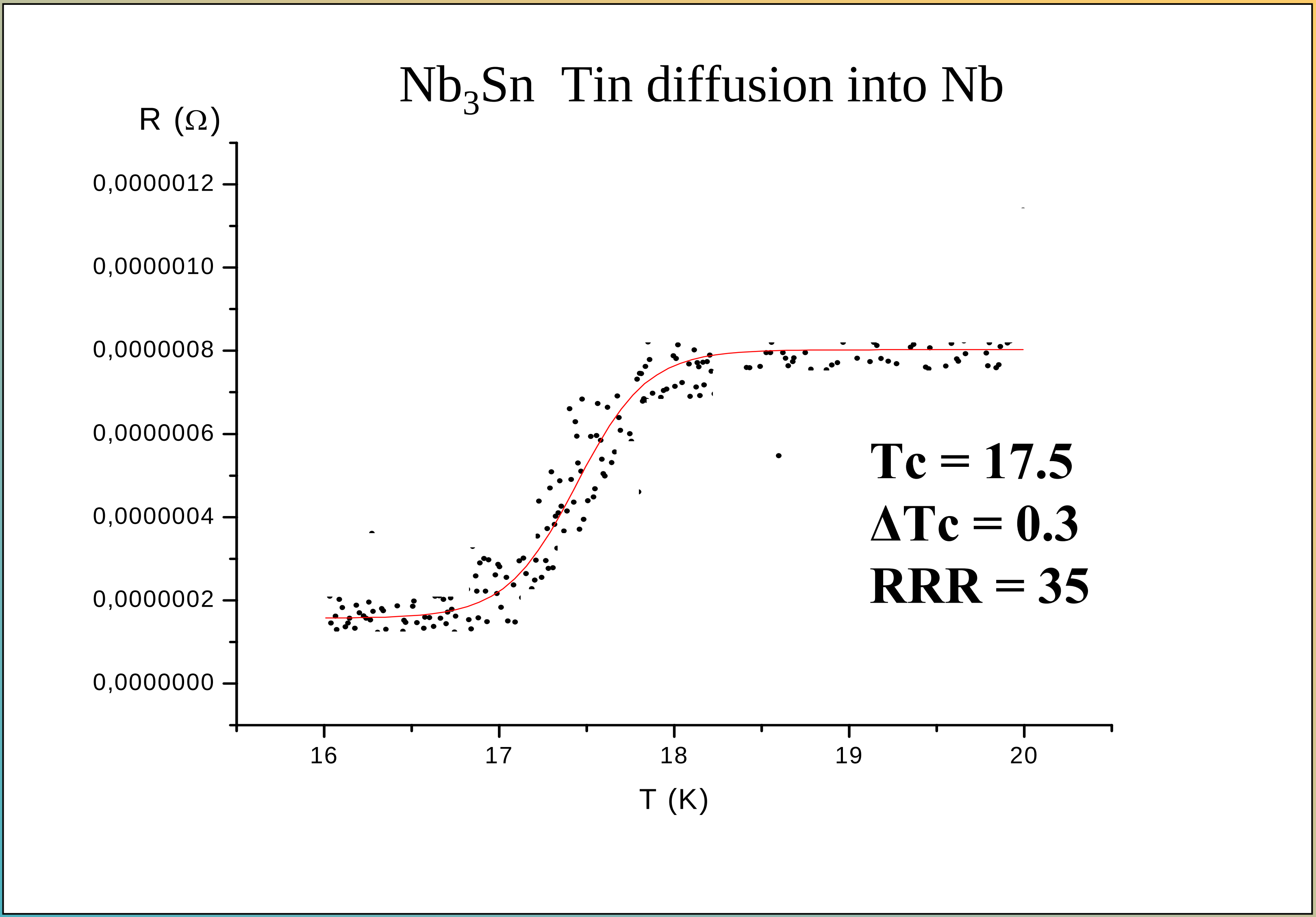

Silvia Deambrosis, Thesis 2004,
Material Science Dept, Padua University

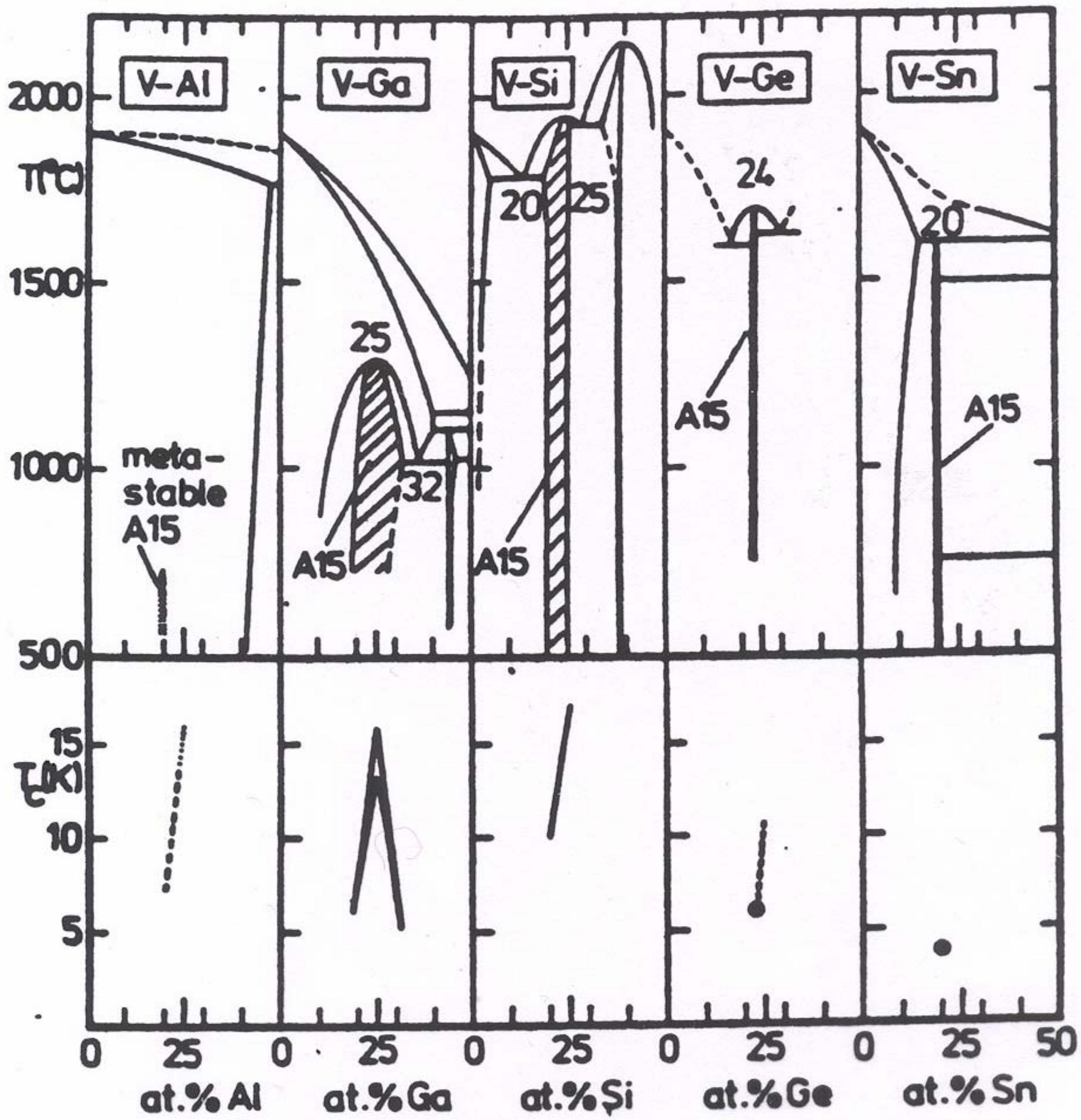
V-Al
V-Ga
V-Si
V-Ge
V-Sn
2000
T(°C)
1500
1000
500
metastable A15
25
32
A15
20
25
24
20
15
T_c(K)
10
5
0
25
50
at.% Al
at.% Ga
at.% Si
at.% Ge
at.% Sn

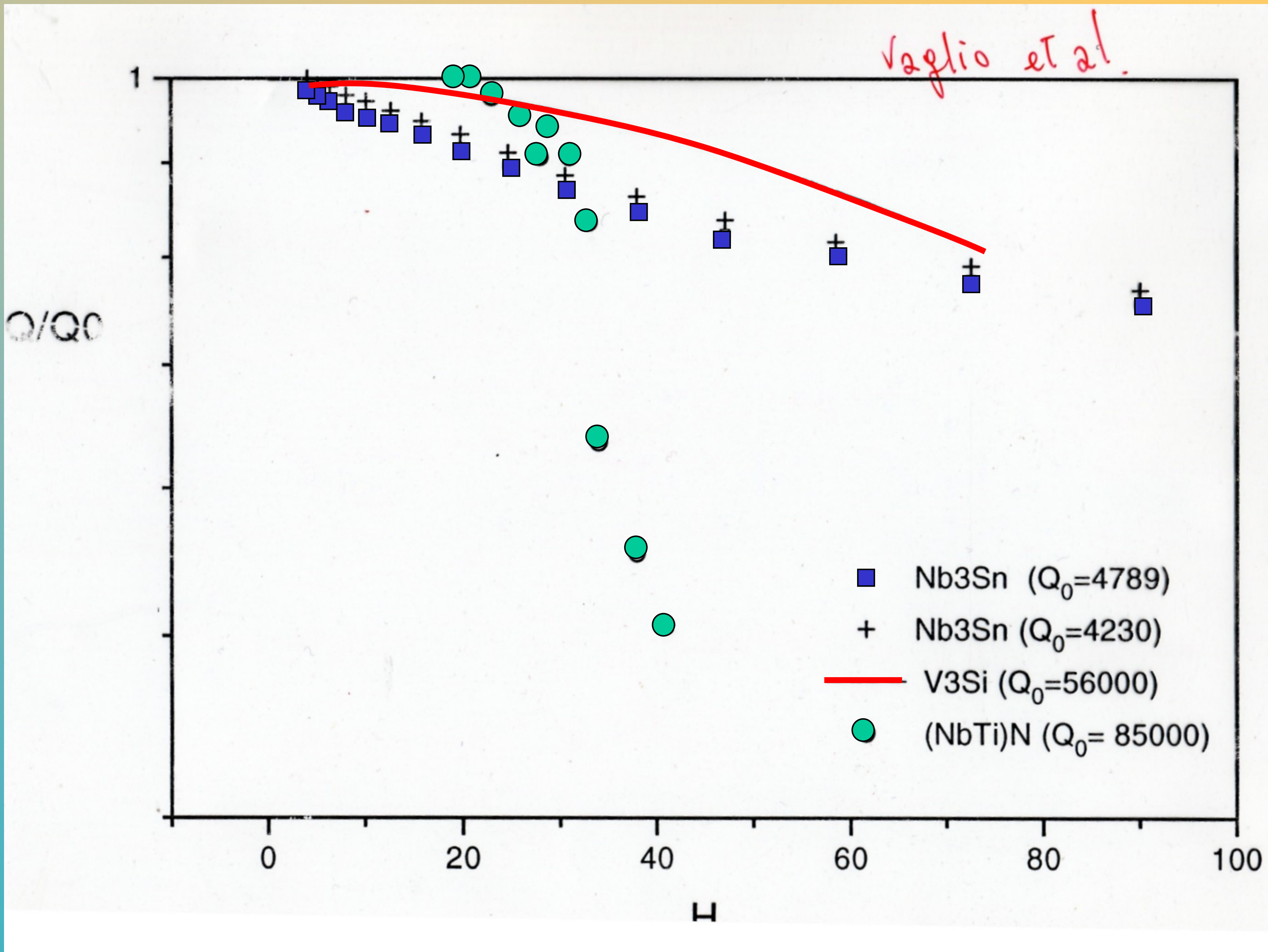
Vaglio et al.
Q/Q0
1
H
0
20
40
60
80
100
Nb3Sn (Q0=4789)
Nb3Sn (Q0=4230)
V3Si (Q0=56000)
(NbTi)N (Q0= 85000)

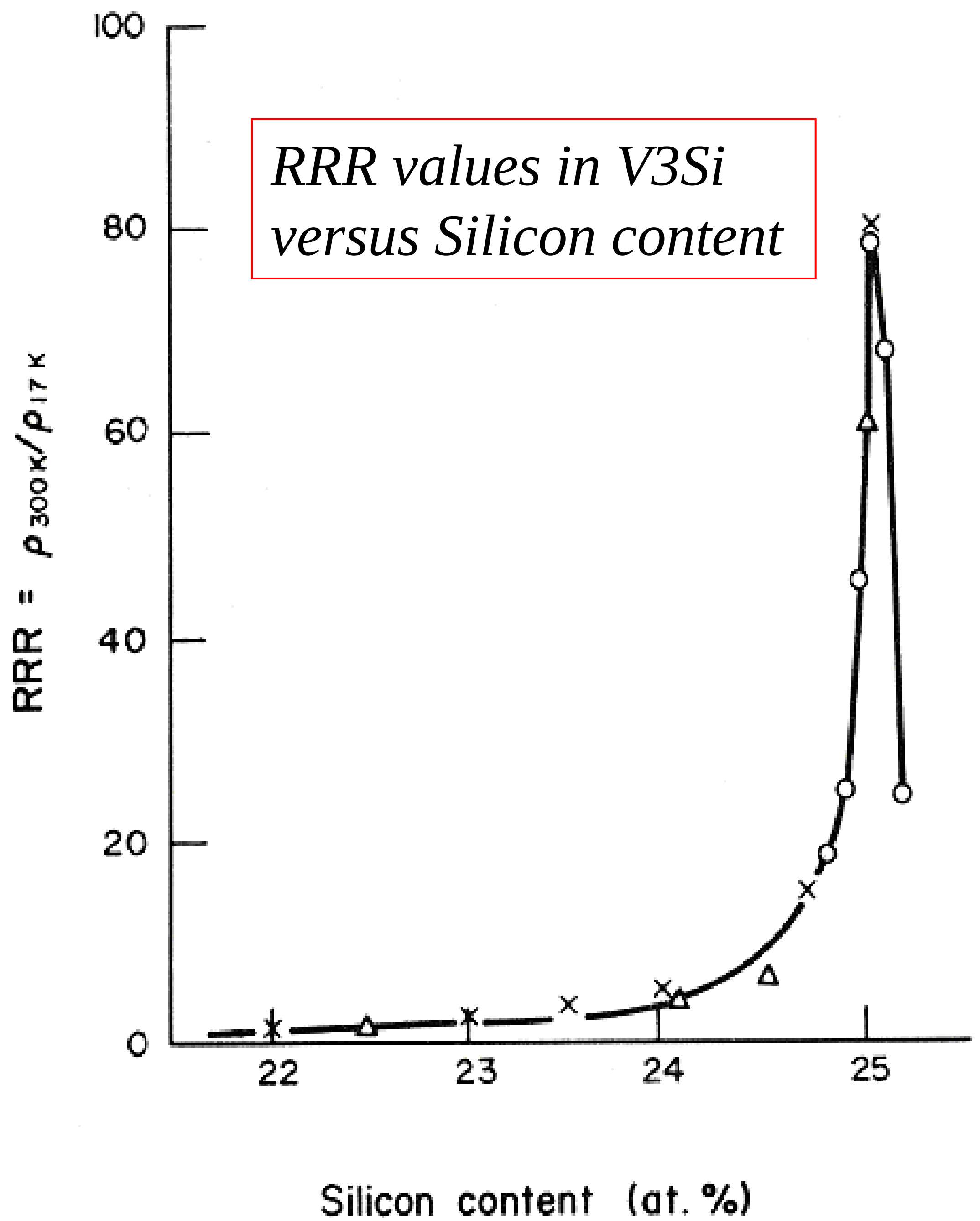
RRR values in V3Si
versus Silicon content
100
80
60
40
20
0
RRR = ρ300K/ρ17K
22
23
24
25
Silicon content (at. %)

Tc vs Si content for sputtered films before and after in situ post-annealing in SiH4 atmosphere

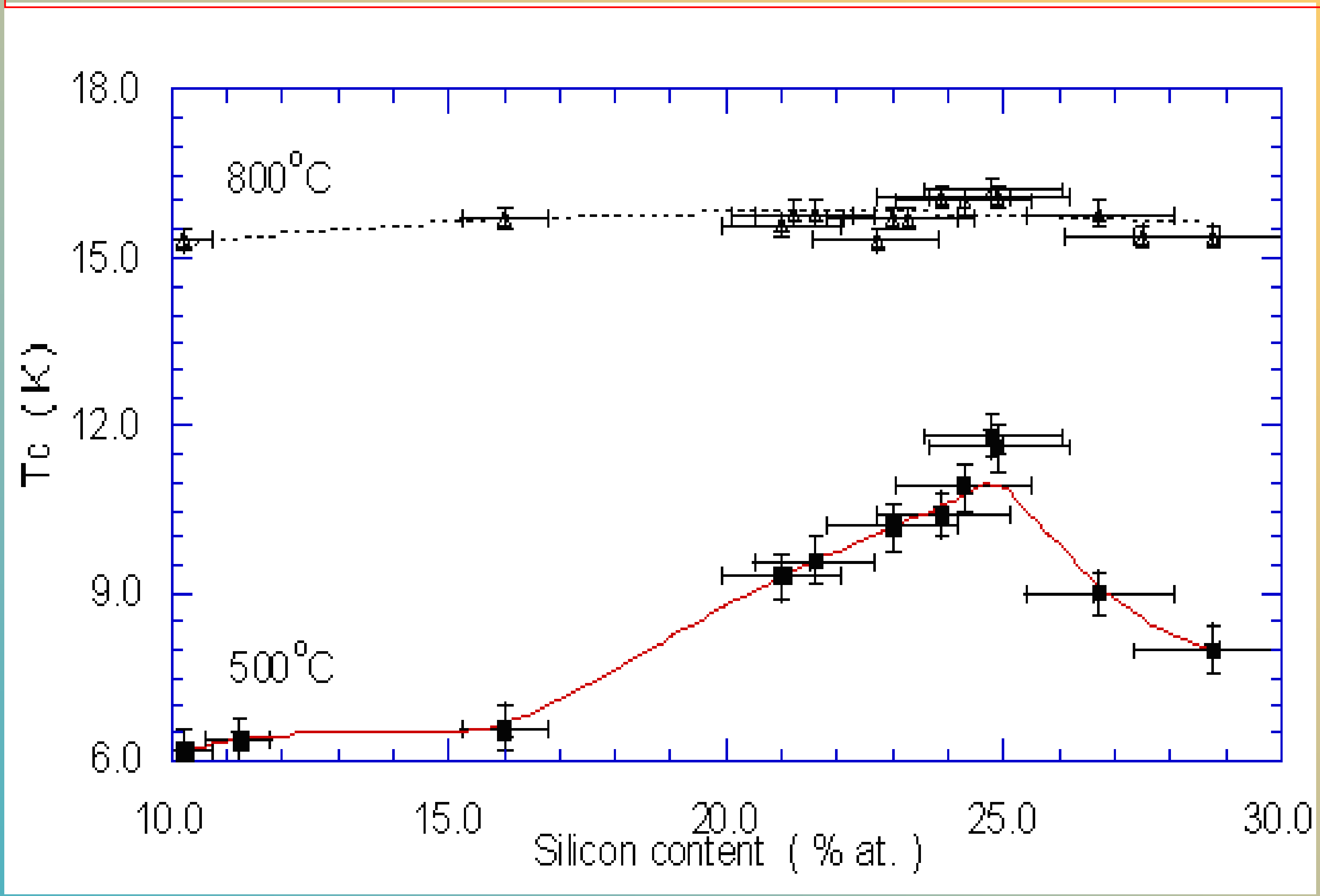

Y. Zhang, V. Palmieri, W. Venturini, F. Stivanello, R. Preciso, **LNL-INFN (REP) 157/2000**

MOCVD of Nb3Sn:

Francesco Todescato, Thesis 2004,
Material Science Dept, Padua University

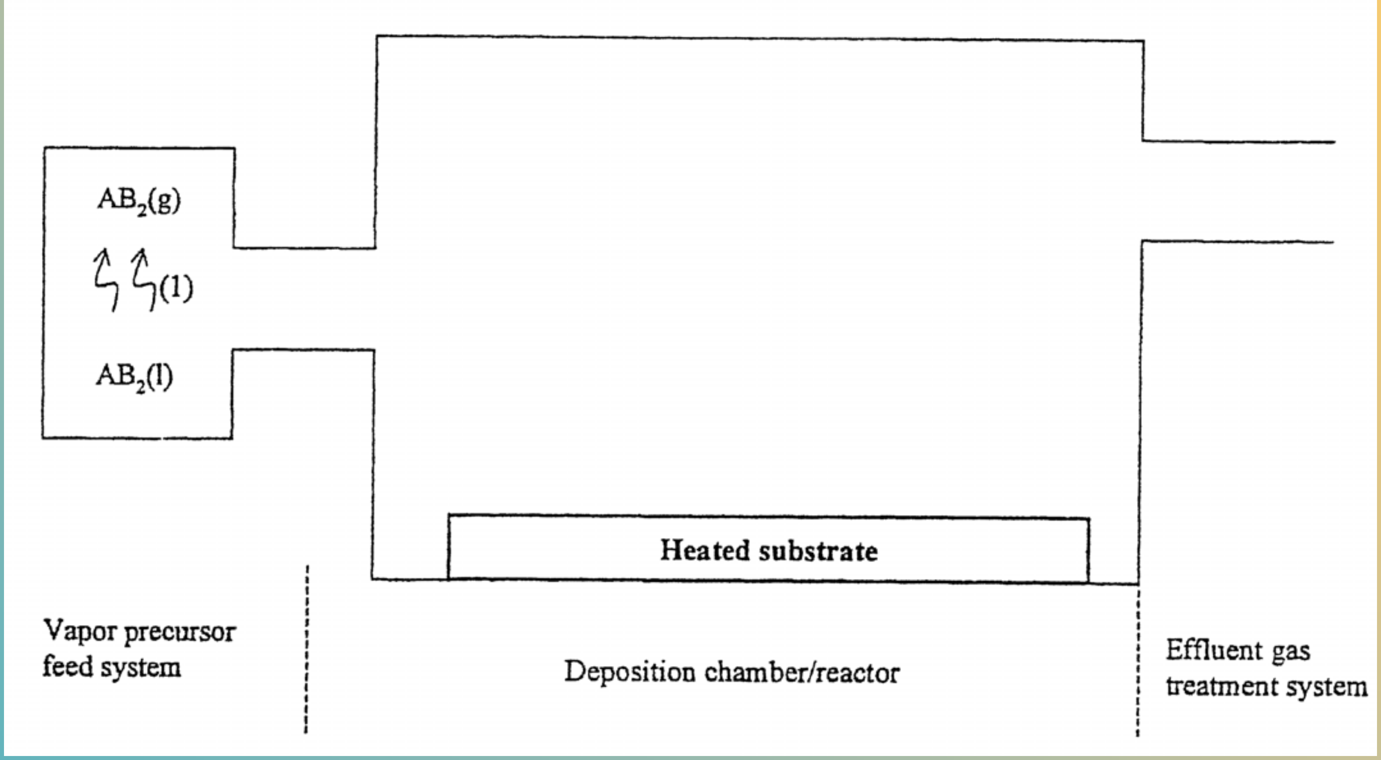

F. Todescato, E. tondello, G. Rossetto, P. Zanella and V. Palmieri,
material still to be published

MOCVD of Nb3Sn:

Francesco Todescato, Thesis 2004,
Material Science Dept, Padua University

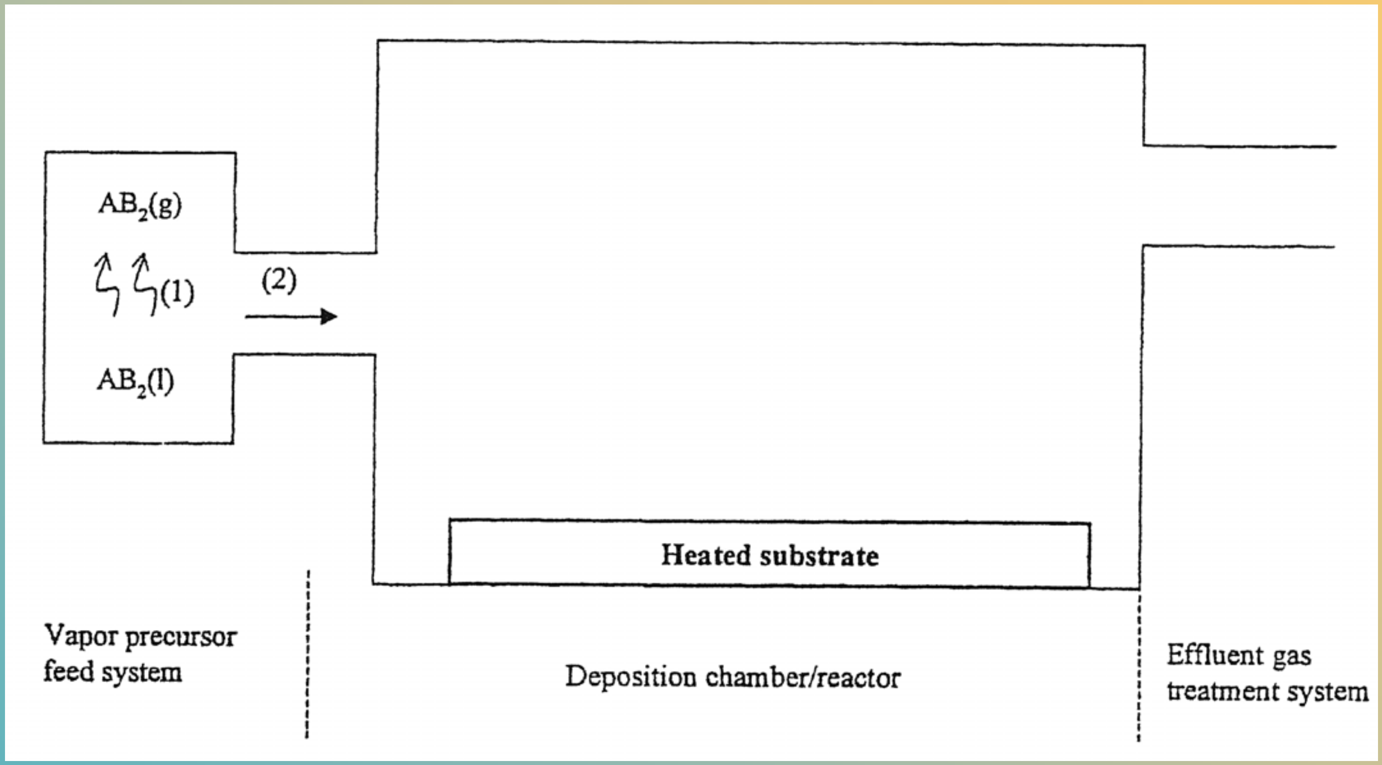

F. Todescato, E. tondello, G. Rossetto, P. Zanella and V. Palmieri, material still to be published

MOCVD of Nb3Sn:

Francesco Todescato, Thesis 2004,
Material Science Dept, Padua University

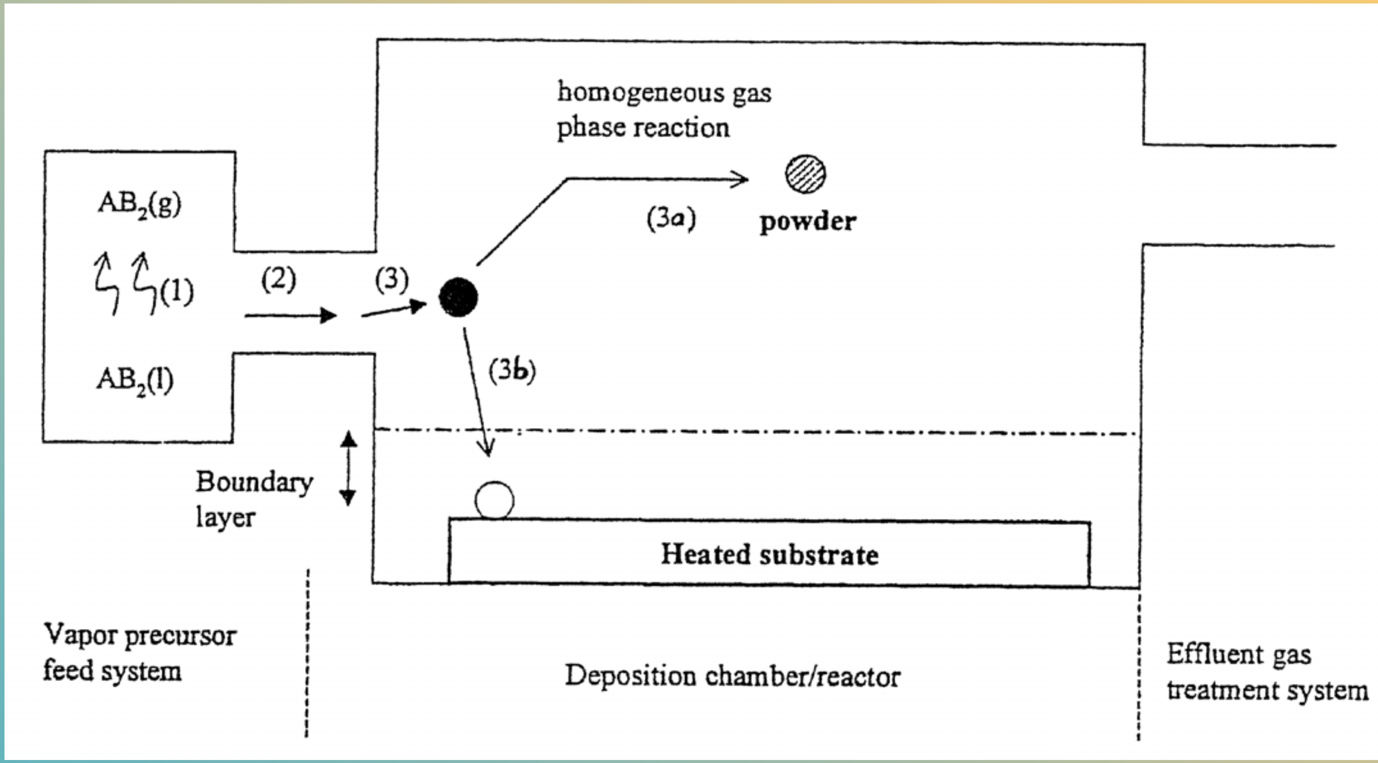

F. Todescato, E. tondello, G. Rossetto, P. Zanella and V. Palmieri, material still to be published

MOCVD of Nb3Sn:

Francesco Todescato, Thesis 2004,
Material Science Dept, Padua University

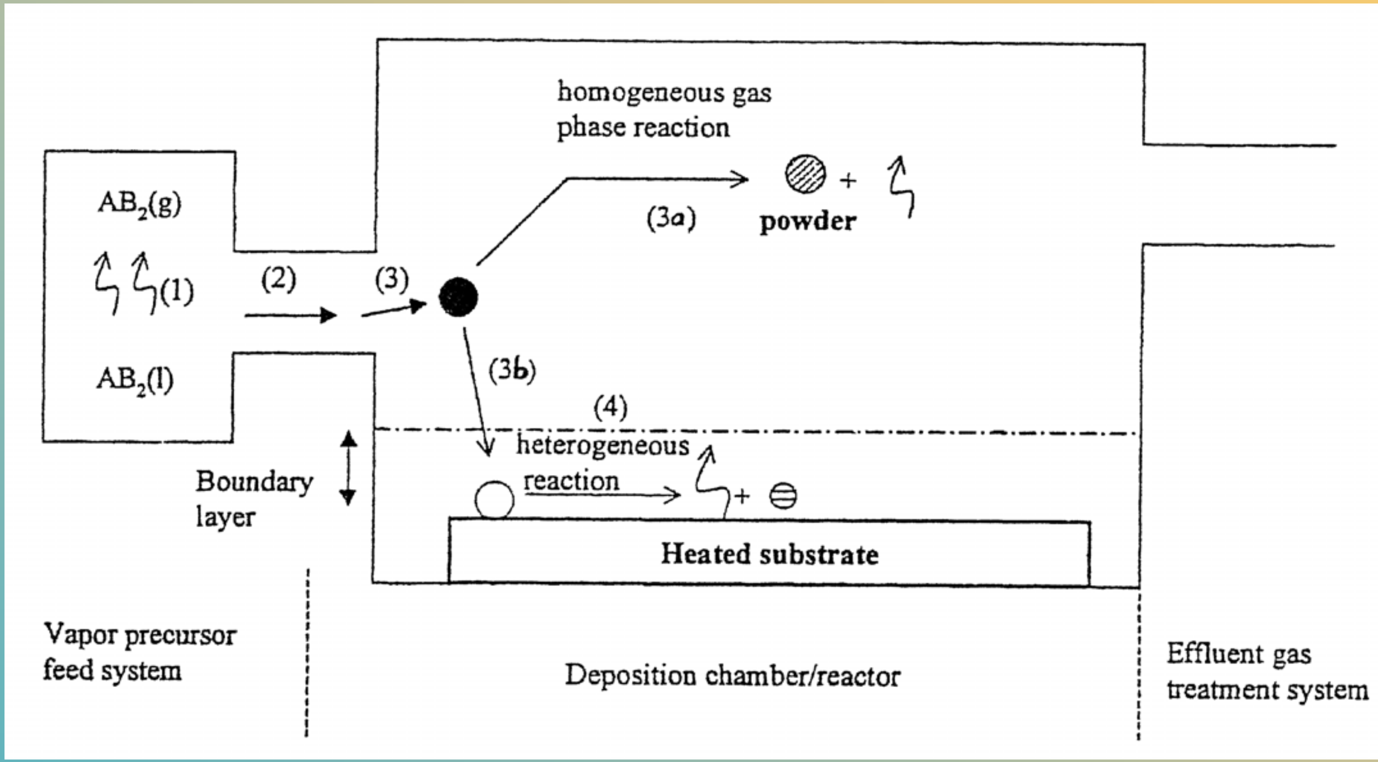

F. Todescato, E. tondello, G. Rossetto, P. Zanella and V. Palmieri, material still to be published

MOCVD of Nb3Sn:

Francesco Todescato, Thesis 2004,
Material Science Dept, Padua University

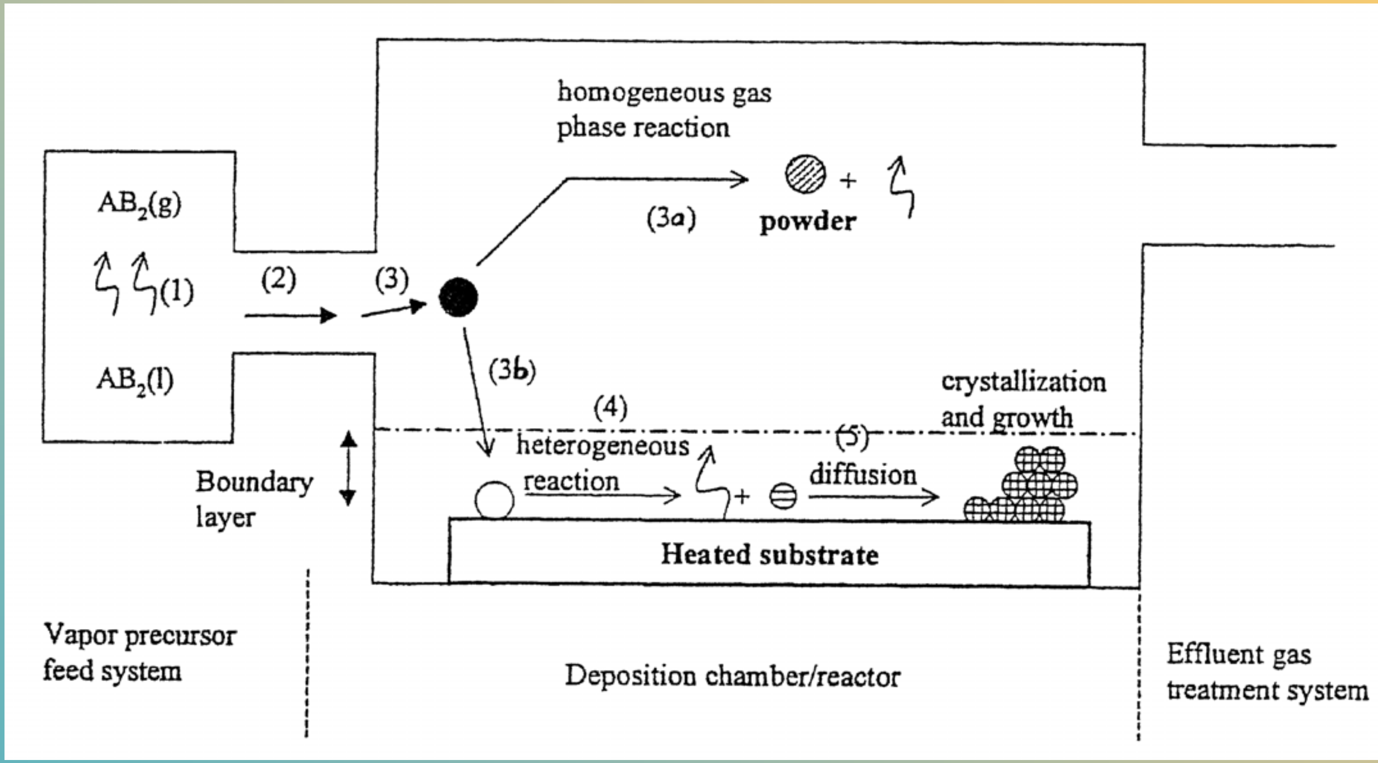

F. Todescato, E. tondello, G. Rossetto, P. Zanella and V. Palmieri, material still to be published

MOCVD of Nb3Sn:

Francesco Todescato, Thesis 2004,
Material Science Dept, Padua University

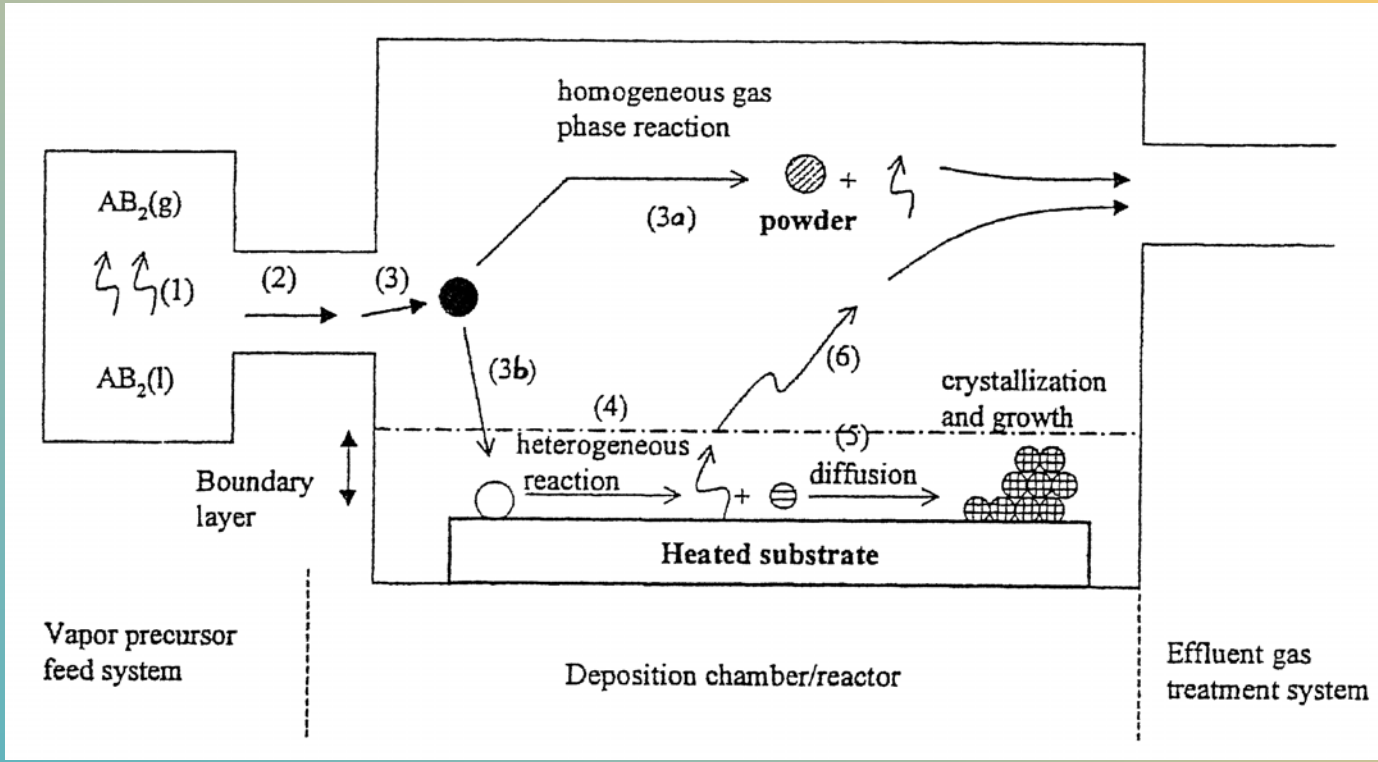

F. Todescato, E. tondello, G. Rossetto, P. Zanella and V. Palmieri, material still to be published

MOCVD of Nb3Sn:

Francesco Todescato, Thesis 2004,
Material Science Dept, Padua University

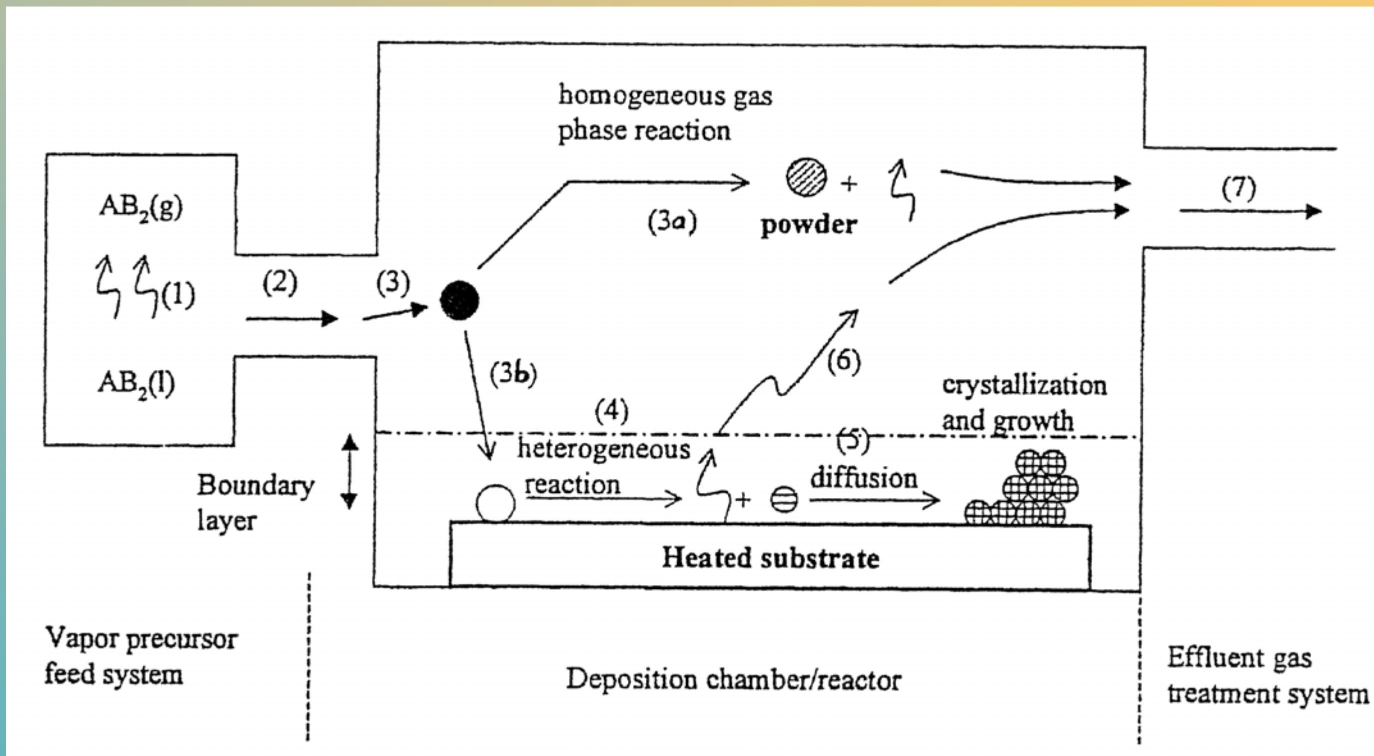

For Nb: several precursors i.e. Niobium pentakis(dimethilammide)
For Sn: Bu3SnH

F. Todescato, E. tondello, G. Rossetto, P. Zanella and V. Palmieri,
material still to be published

Francesco Todescato, Thesis 2004,
Material Science Dept, Padua University

Synthesis of Niobium Pentakis(dimethilammide)

The reaction happens in two different steps:

First the Me_2NH 50 mL is bubbled for around 90 minutes in LiBu:

$$Me_2NH + LiBu \rightarrow LiNMe_2 + BuH$$

Than the butane is evaporated and the product obtained is suspended in pentane and treated by $NbCl_5$

$$NbCl_5 + 5LiNMe_2 \xrightarrow{\text{pentane}} Nb(NMe_2)_5 + 5LiCl$$

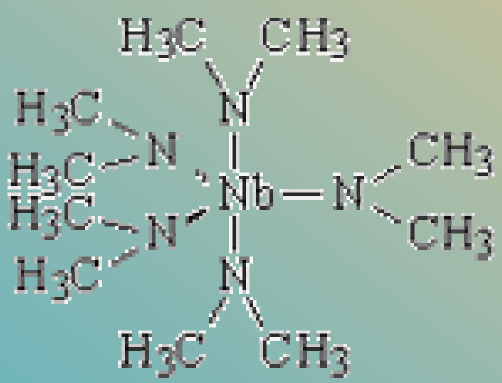

The Ammide is a brrownish powder that sublimes at 130°C

RBS del deposito 1 da $CpNbMe_4$

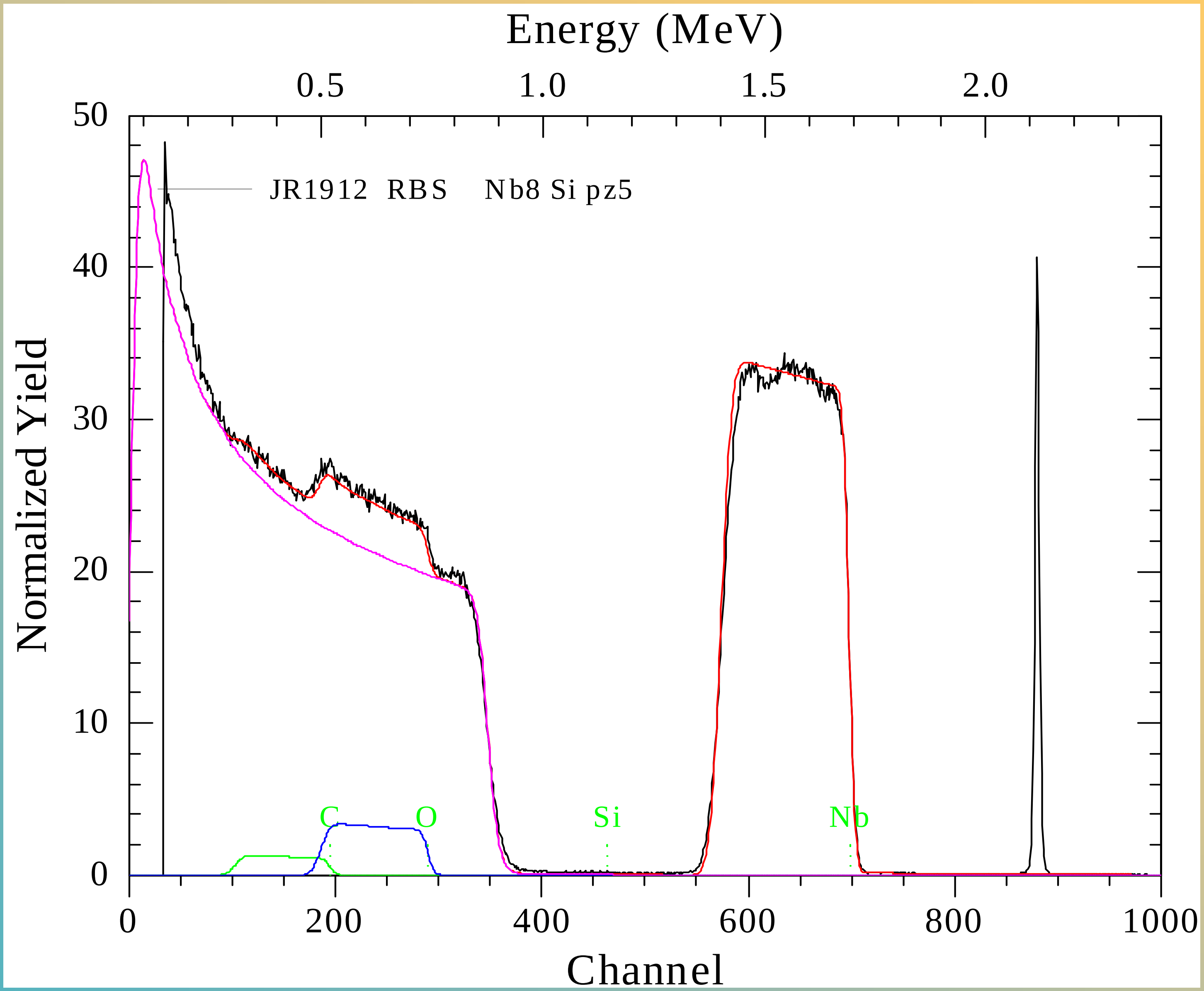

Rapporti relativi:

Nb = 1,00

O = 2,38

C = 1,58

A possible source of oxygen contamination

Molybdenum-Rhenium

Most commonly known as **Moly-Rhenium**, and used extensively throughout many industries -from medicine to defense and pure research to production welding, this material is a less costly alternative to pure rhenium.

Possessing excellent thermal and mechanical properties, **Moly-Rhenium** is used as welding wire, wires for numerous medical applications, components and parts for the aerospace and defense industries, and grids for electronic applications.

Density, g/cm^3	13.52
Melting Point, °C	2550
Thermal Conductivity, W/m at 20°C	36.8
Linear Coefficient of Thermal Expansion, µm/m·K from 20-1000°C	5.7
Ductile Brittle Transition Temperature (DBBT), °C	(-273)-(-173)
Critical Superconducting temperature, K	10.9
Electrical Resistivity, µΩ·m at 20°C	0.220
Elastic Modulus in Tension, GPa	373

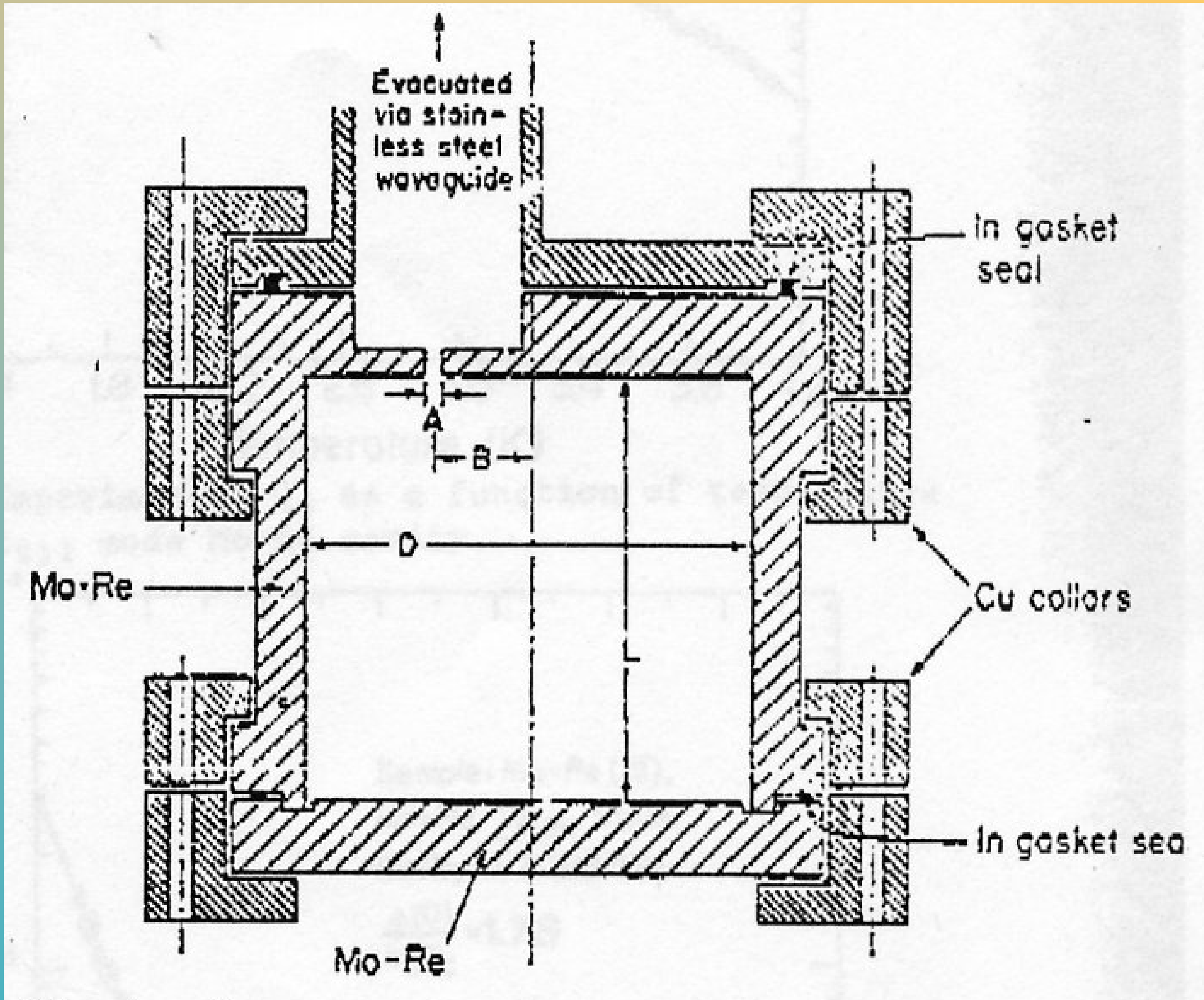

Evacuated via stainless steel waveguide
In gasket seal
A
B
D
L
Mo-Re
Cu collars
In gasket sea
Mo-Re

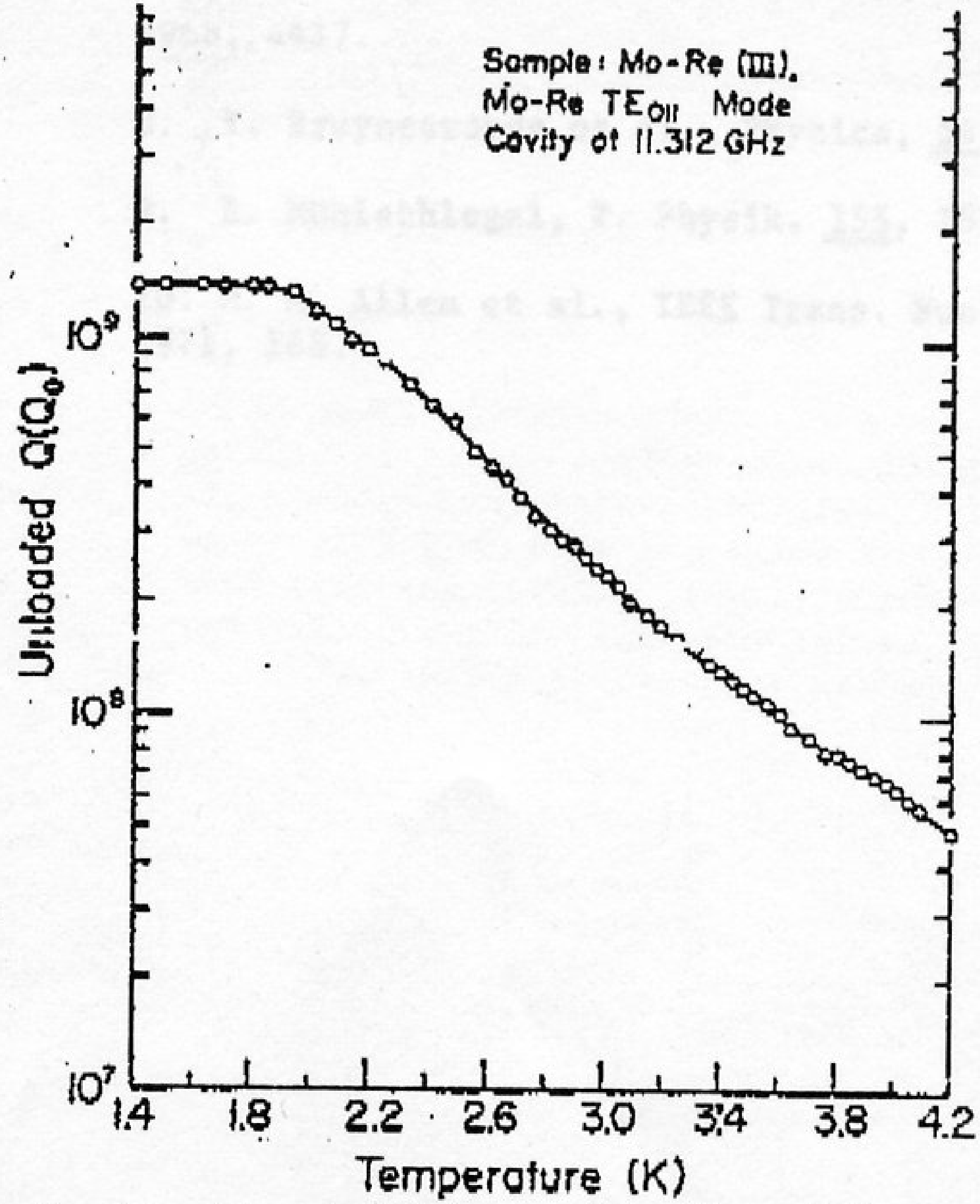

Fig. 4. Experimental Q_o as a function of temperature for the TE_{011} mode Mo-Re cavity.

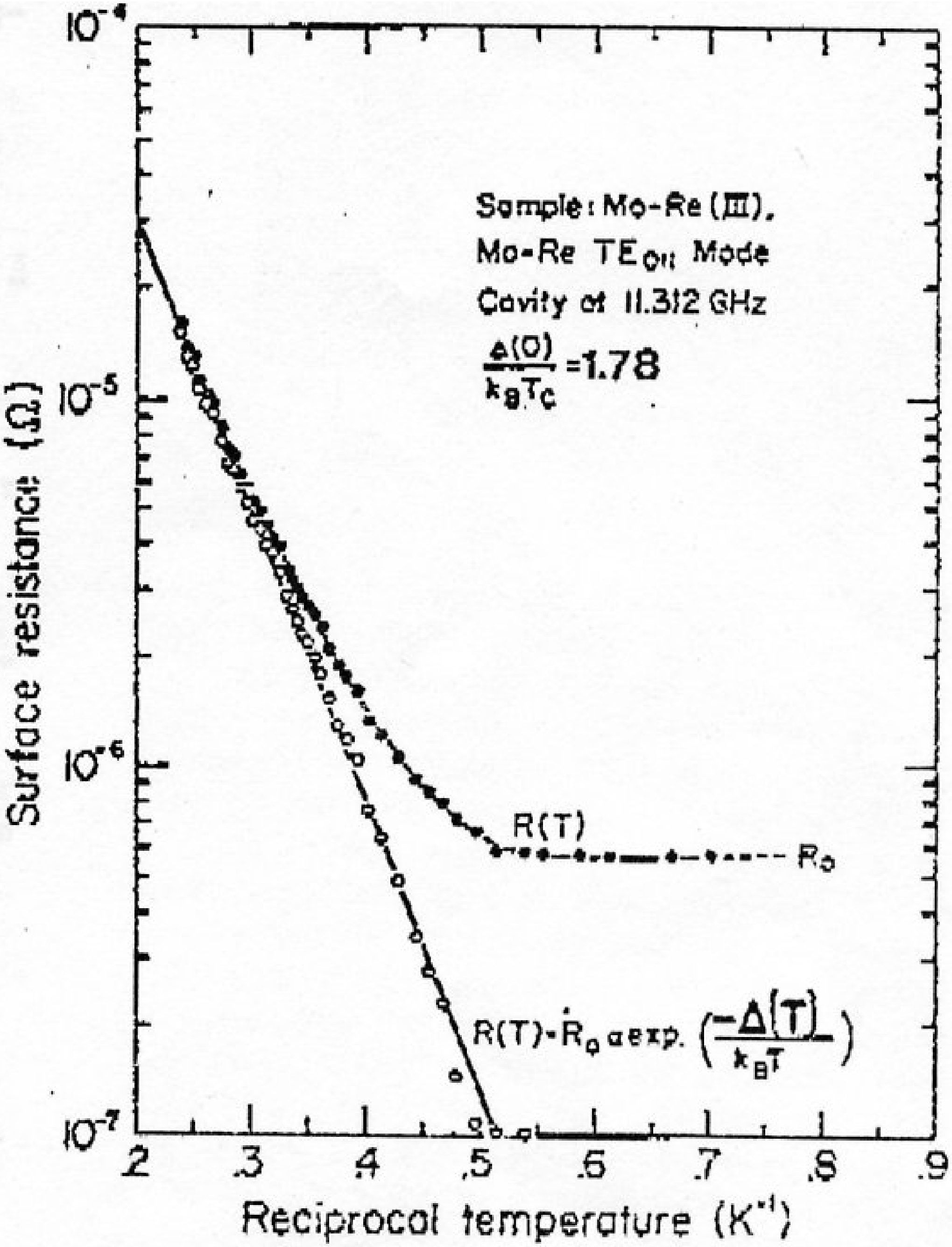

Fig. 5. Experimental surface resistance as a functio[n] of reciprocal temperature.

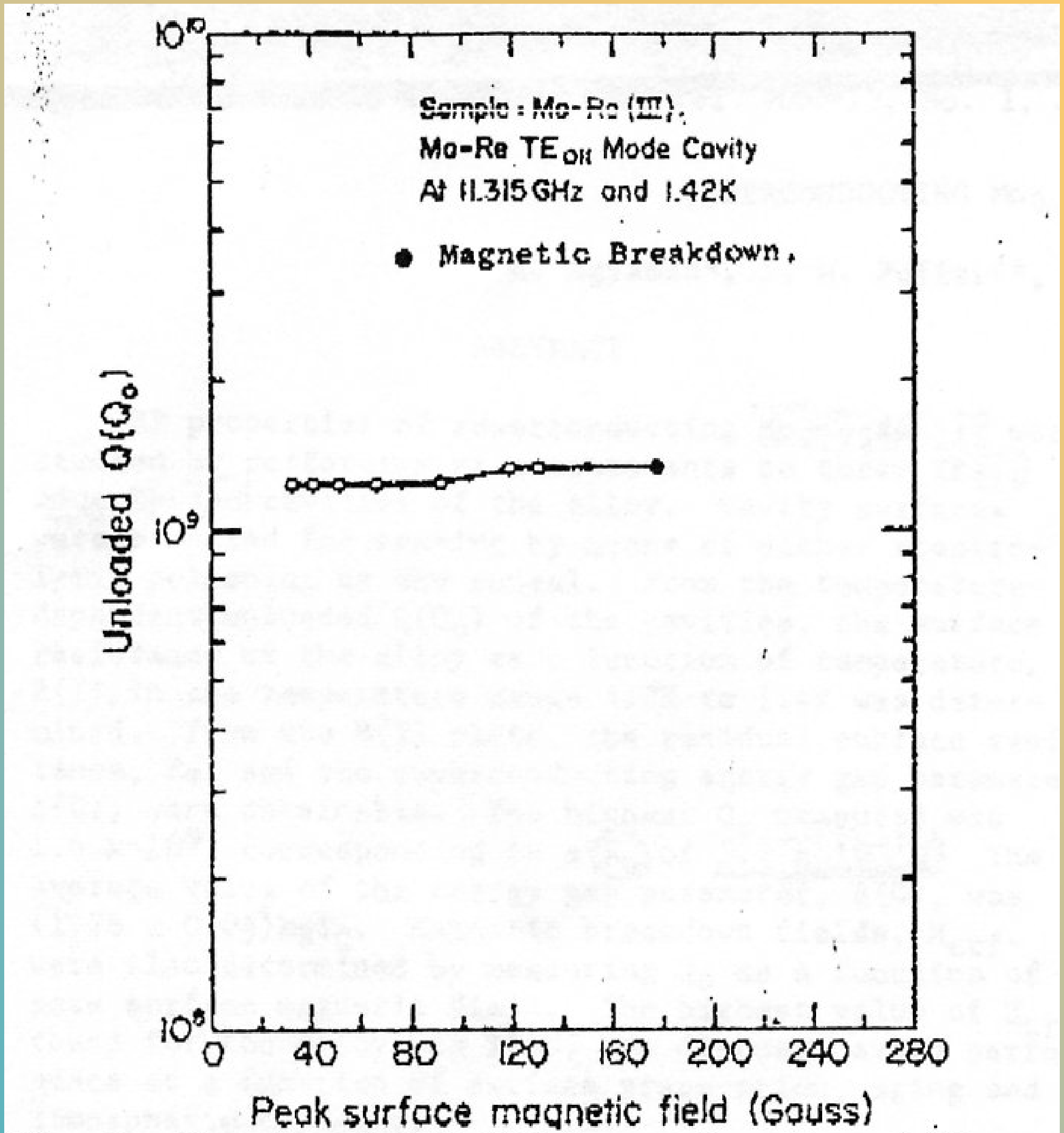

Fig. 6. Example of unloaded Q as a function of Rf magnetic field.

(After Yasaitis and Rose, 1975)

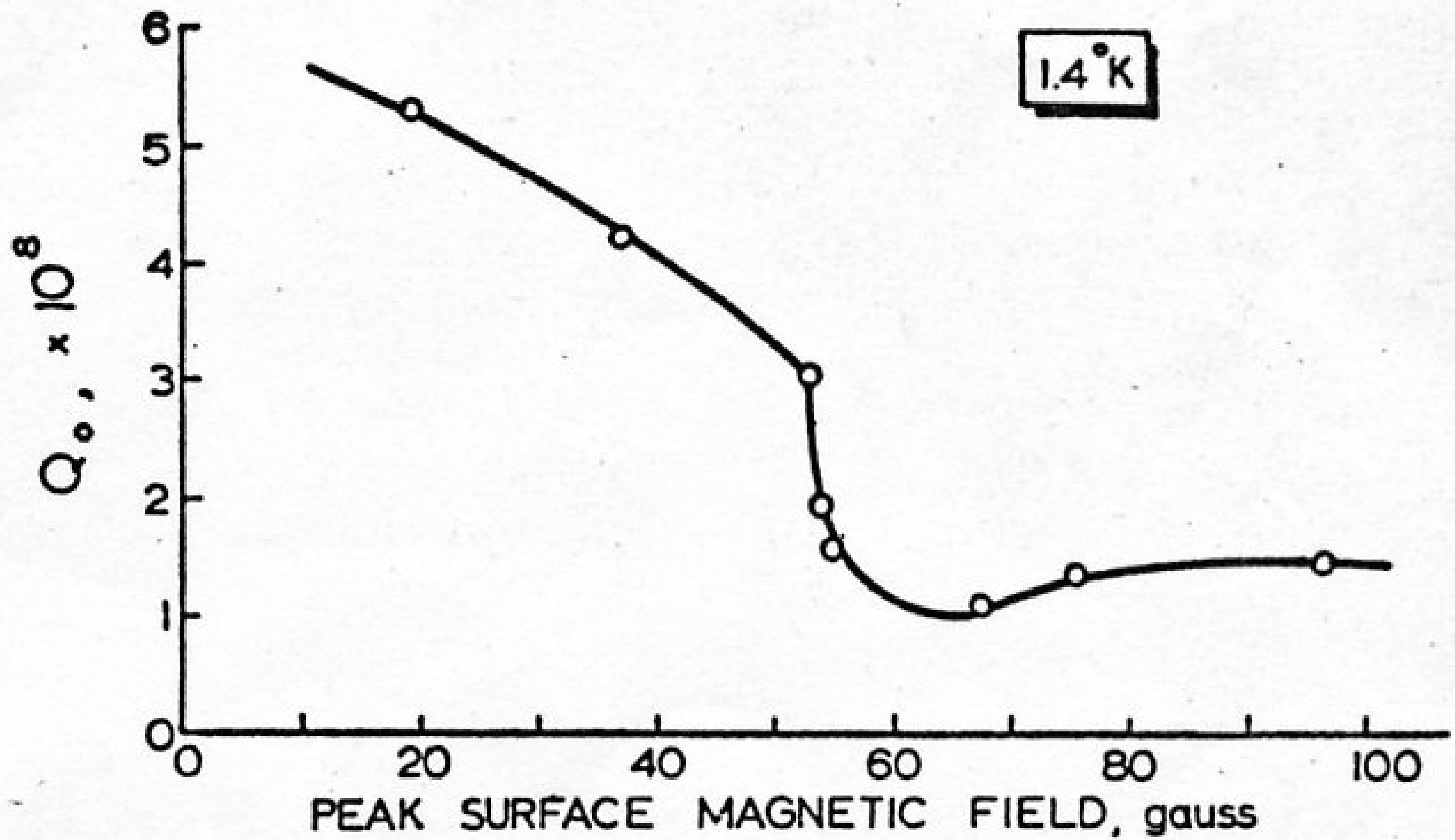

Fig. 2. High-power measurement on composite (Nb + Mo-Re) cavity.

Nb_3Sn 1.5GHz cavity made at Wuppertal by Sn vapour phase diffusion

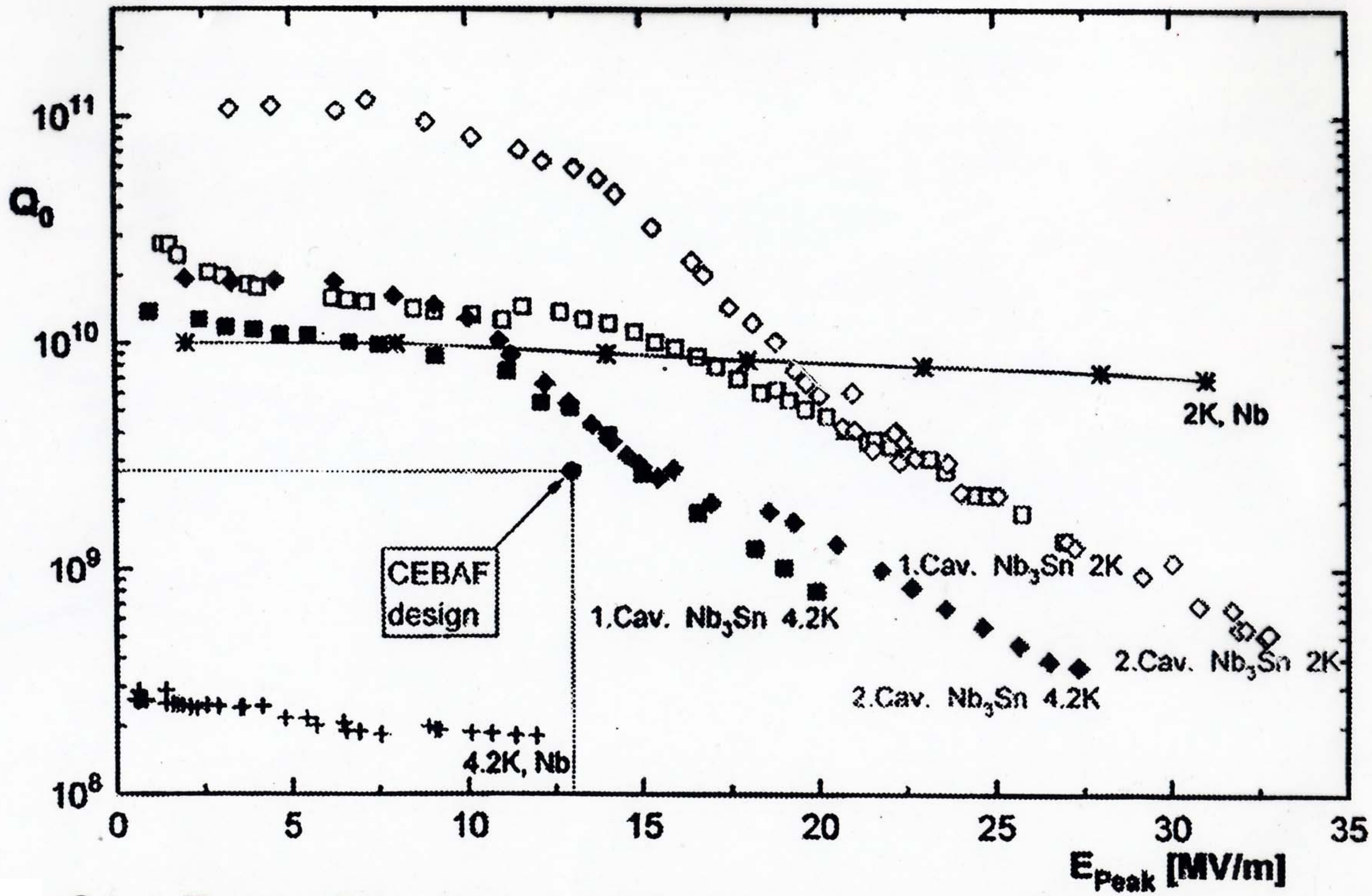

Q vs. Epeak of the first two Nb3SN-coated 1.5 GHz single-cell cavites in comparison to pure Nb at 4.2 K and 2 K from CEBAF.

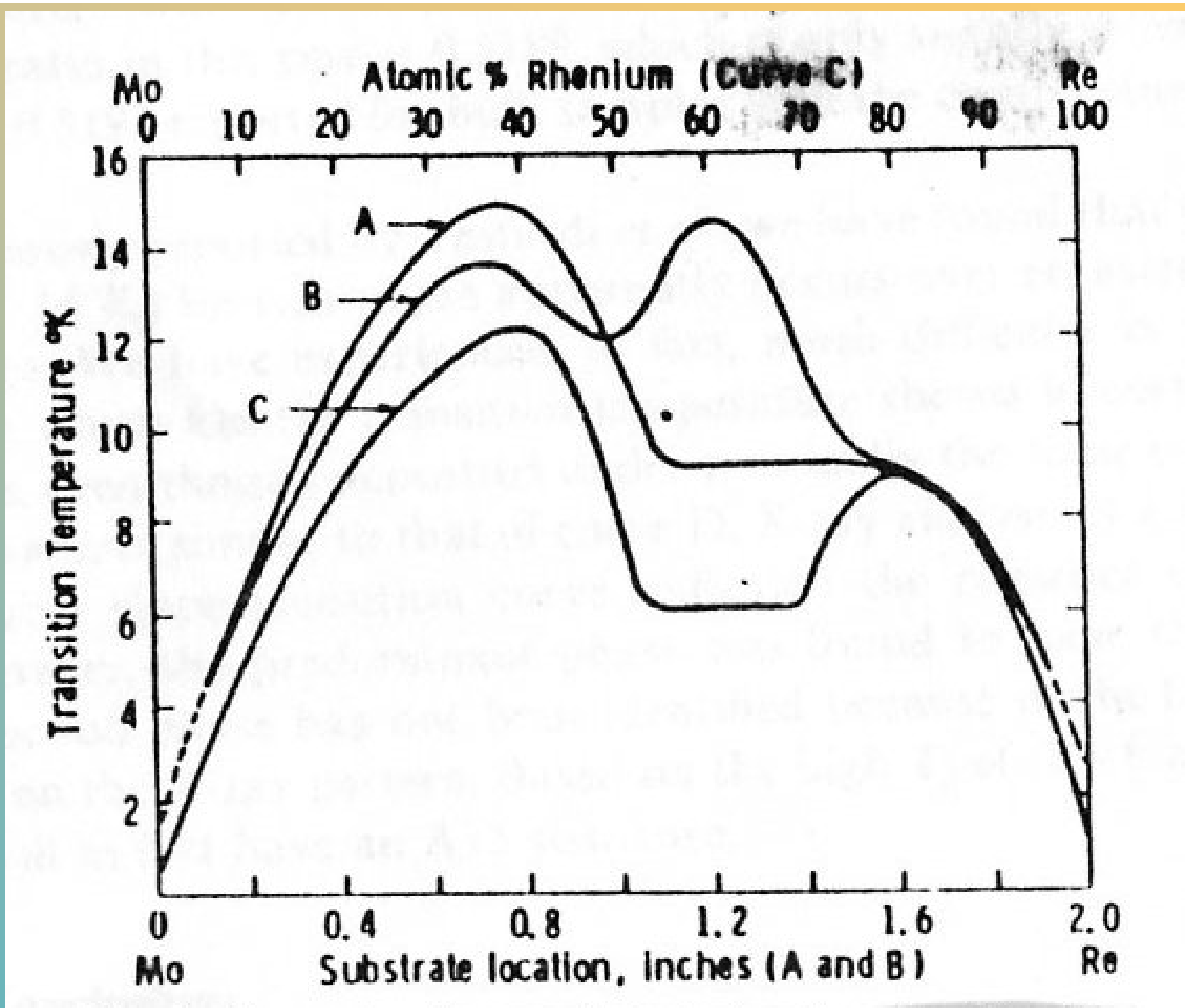

Curve **A** - Films sputtered at ~ **500 Å/min** onto **1000 °C** substrates

Curve **B** – Films sputtered at ~ **1000 Å/min** onto **1200 °C** substrates

Curve **C** – Bulk Mo-Re samples

From Blaugher et al

$Mo_{38}Re_{62}$ (after Testardi)

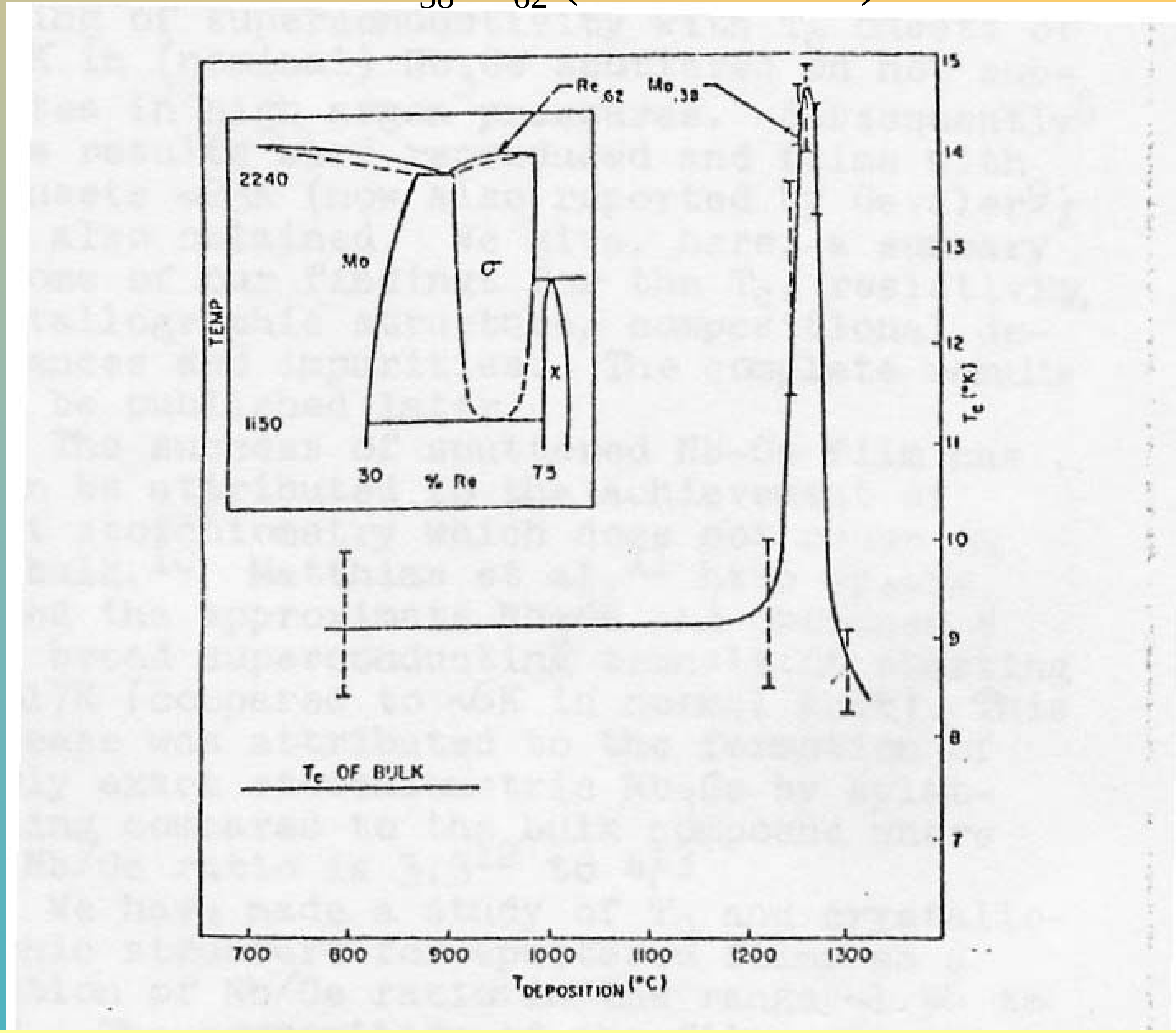

(The author communicates that the Temperature was 150 C lower than reported in the picture)

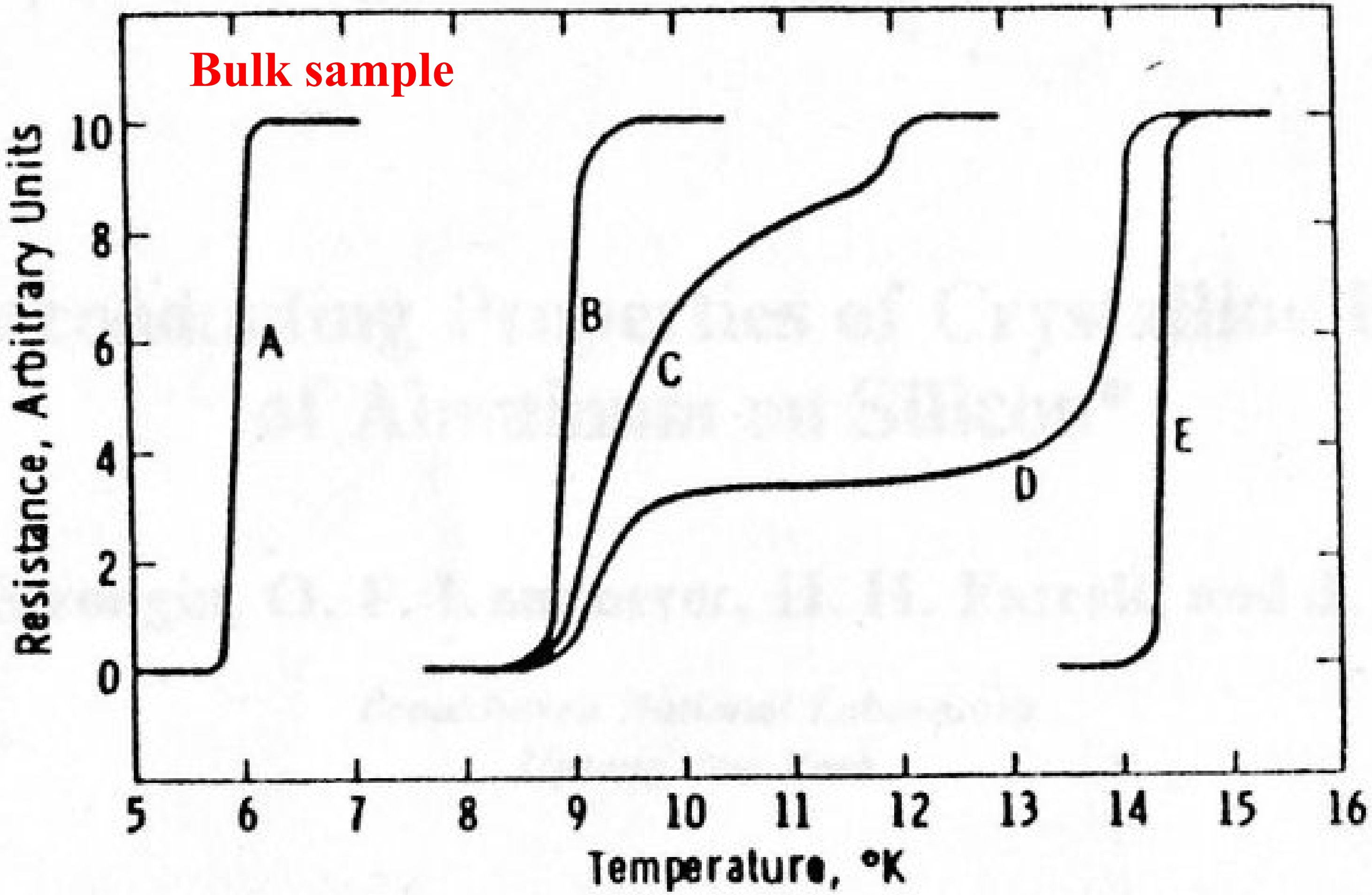

Fig. 3. T_c's of Mo–Re alloy samples all of the approximate composition $Mo_{40}Re_{60}$. A—Bulk sample[4]; B, C, D, E—thin films sputtered at ~ 1000 Å/min onto 600°C, 750°C, 1150°C, and 1200°C substrates, respectively.

$$R_S = R_S\,(e^{-sT_c/2T})$$

Measured Parameters of V1-B, VII-B Superconductors

Compound	γ(mJ/g-atom-K^2)	β(mJ/g-atom-K^4)	δ(mJ/g-atom-K^6)	θ_D(K)	$2\Delta/kT_c$	T_c onset	Struct.
$Mo_{0.6}Re_{0.4}$	4.55	.05639	.0001535	325	5.0	12.0	bcc
	4.44	.0481	–	340	–	12.6	bcc
$Mo_{0.4}Re_{0.6}$	3.60	.04881	0	342	3.4	6.0	tetr.
	3.2	–	–	355	–	6.49	tetr.
$Mo_{0.42}Re_{0.58}$	3.31	–	–	351	2.8	6.35	tetr.
$Mo_{0.23}Re_{0.77}$	3.8	–	–	272	3.0	9.25	A-12
$W_{0.65}Re_{0.35}$	2.49	.06599	0	309	3.1	6.75	bcc
$W_{0.80}Re_{0.20}$	2.2	–	–	359	–	–	bcc
$W_{0.75}Re_{0.25}$	2.3	–	–	351	–	–	bcc
$W_{0.59}Re_{0.50}$	2.69	–	–	327	3.3	5.12	tetr.
$Mo_{0.18}Tc_{0.82}$	8.	.03396	.0002317	385	3.6	13.7	hcp

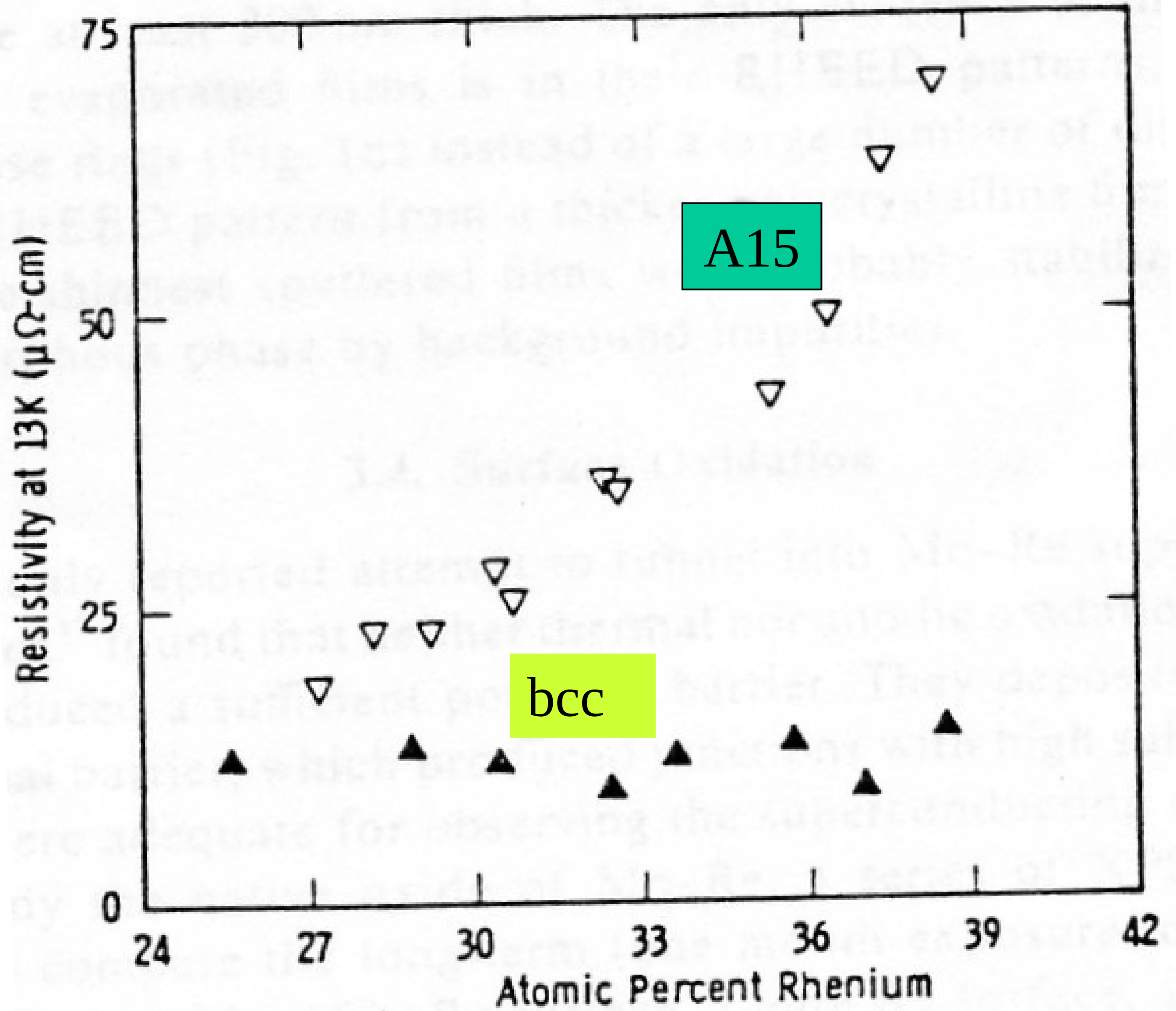

Normal-state resistivity plotted as a function of Re composition for films with A15 and α-Mo structures.

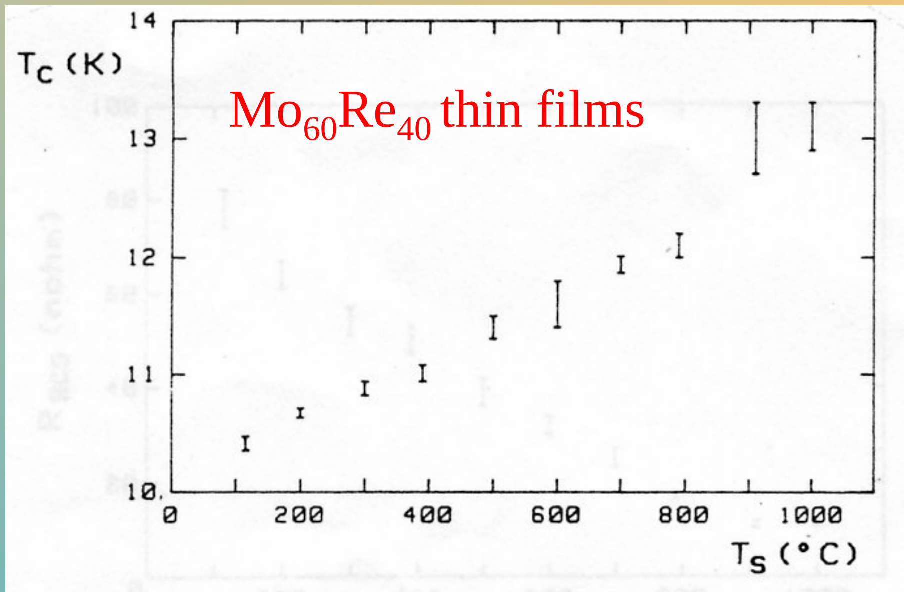

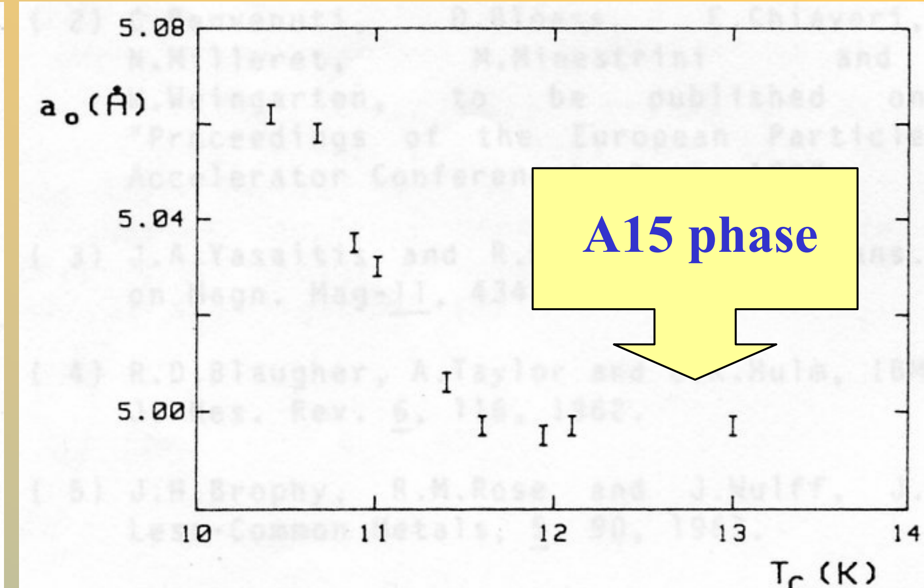

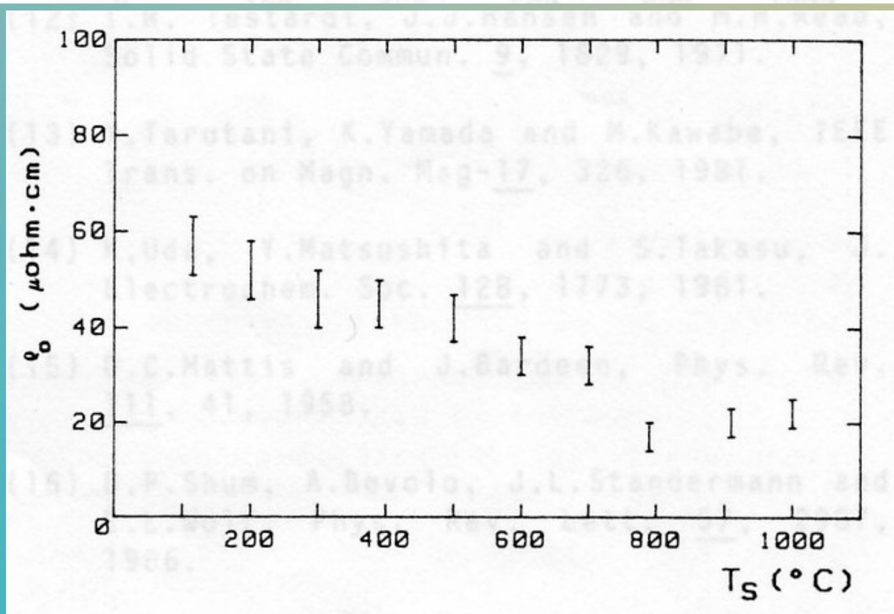

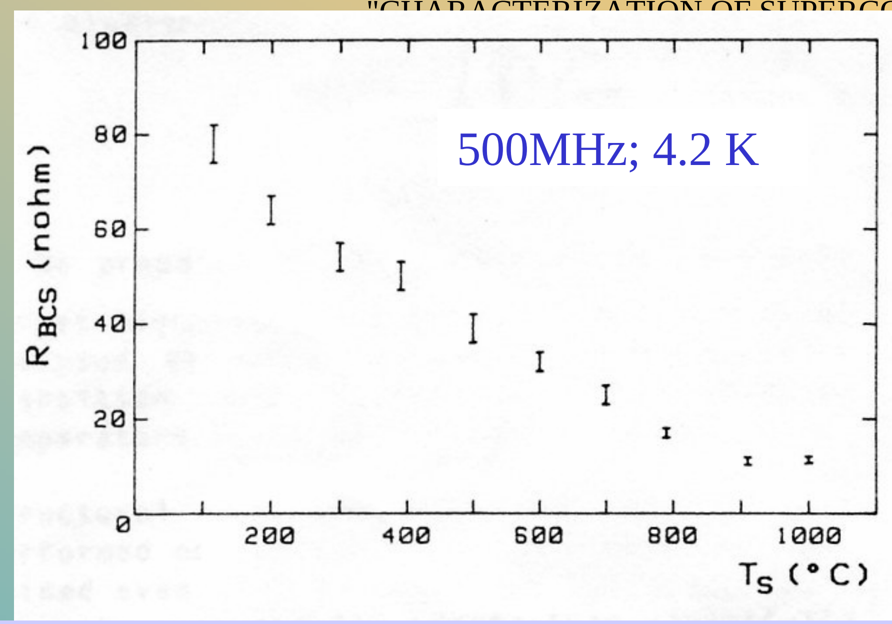

A.Andreone, A.Barone, A.Di Chiara, G.Mascolo, V.Palmieri, G.Peluso, U.Scotti, "Mo-Re Superconducting Thin Films by Single Target Magnetron Sputtering", **IEEE Trans. Mag., 25, 2, (1989) 1972**

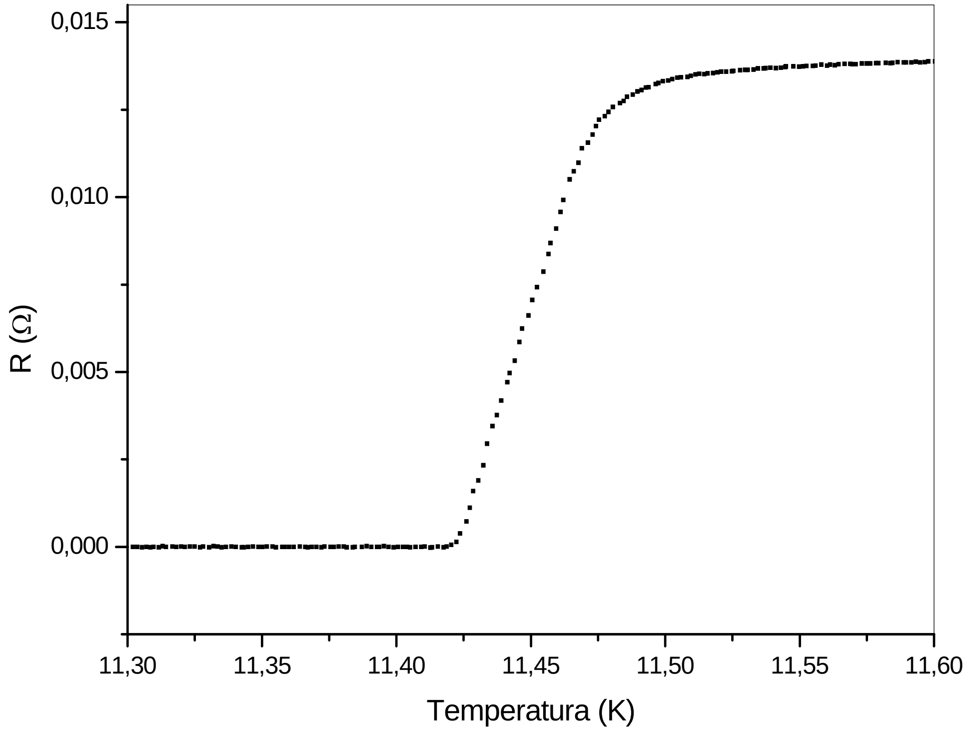

Sputtered films from $Mo_{75}Re_{25}$ arc melted target

$\Delta T_C = 0.02$ K

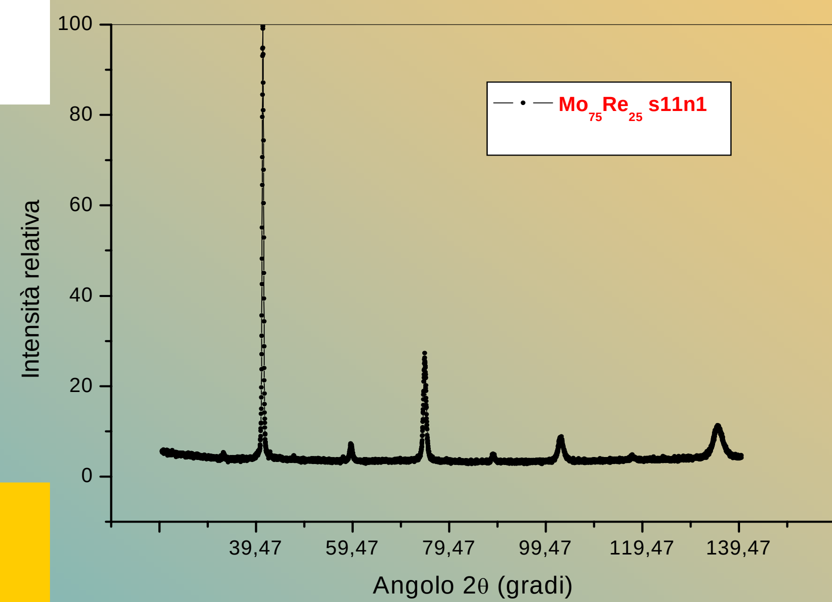

Silvia Deambrosis, Thesis 2004,
Material Science Dept, Padua University

A 6 GHz seamless cavity

A cheap way to fabricate samples for RF properties from Nb retails

15 minutes of fabrication time, including flanges,

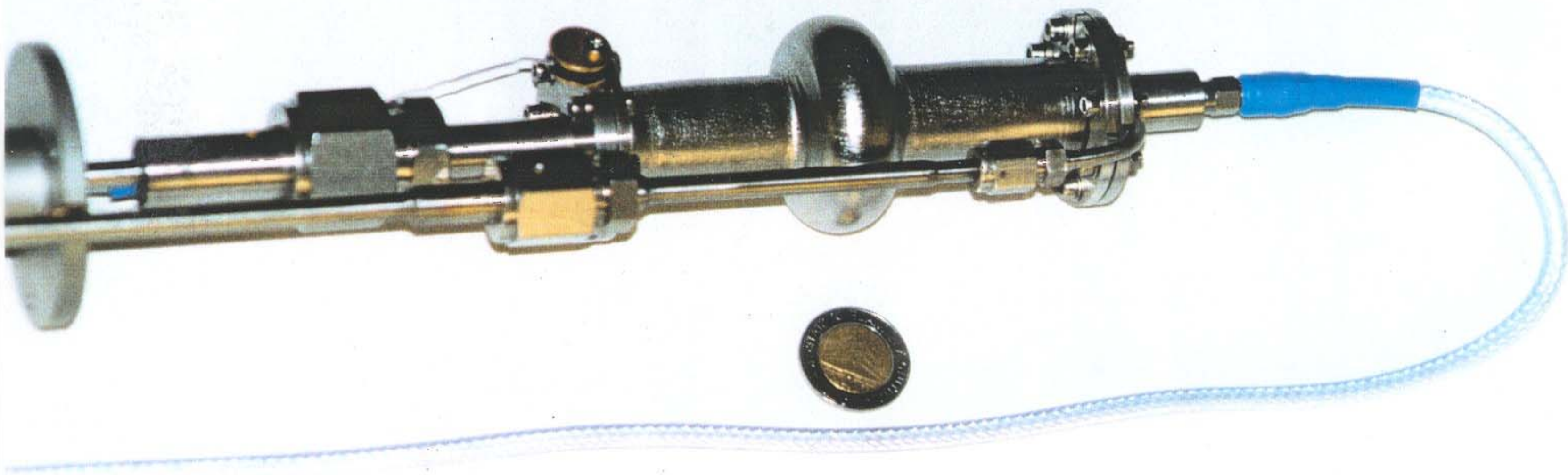

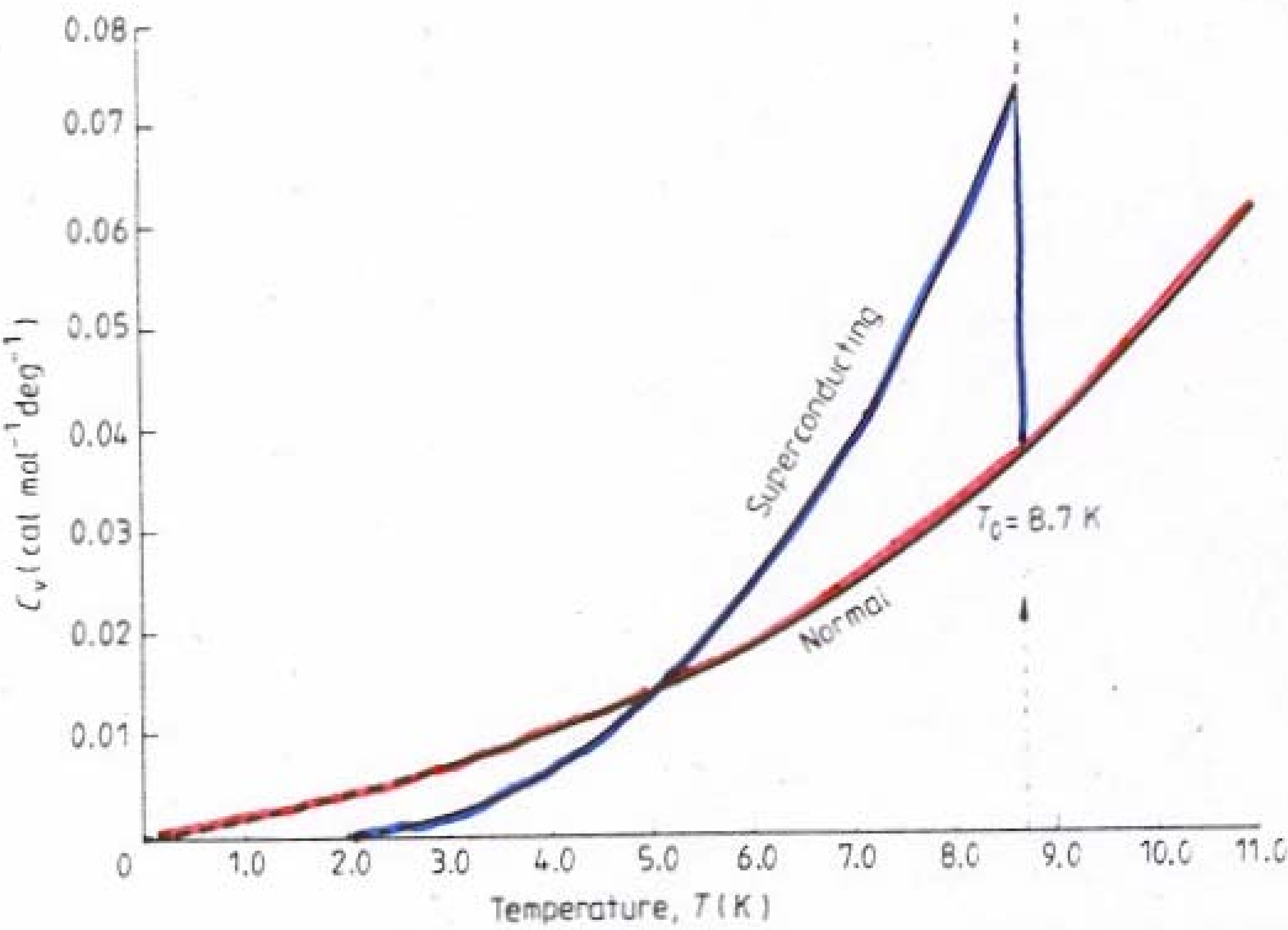
0.08
0.07
0.06
0.05
0.04
0.03
0.02
0.01
0
1.0
2.0
3.0
4.0
5.0
6.0
7.0
8.0
9.0
10.0
11.0
C_v (cal mol^{-1} deg^{-1})
Temperature, T (K)
Superconducting
Normal
T_c = 8.7 K

Specific heat measurement

Surface Resistance measurement

In both cases we measure the Boltzman' Exponential

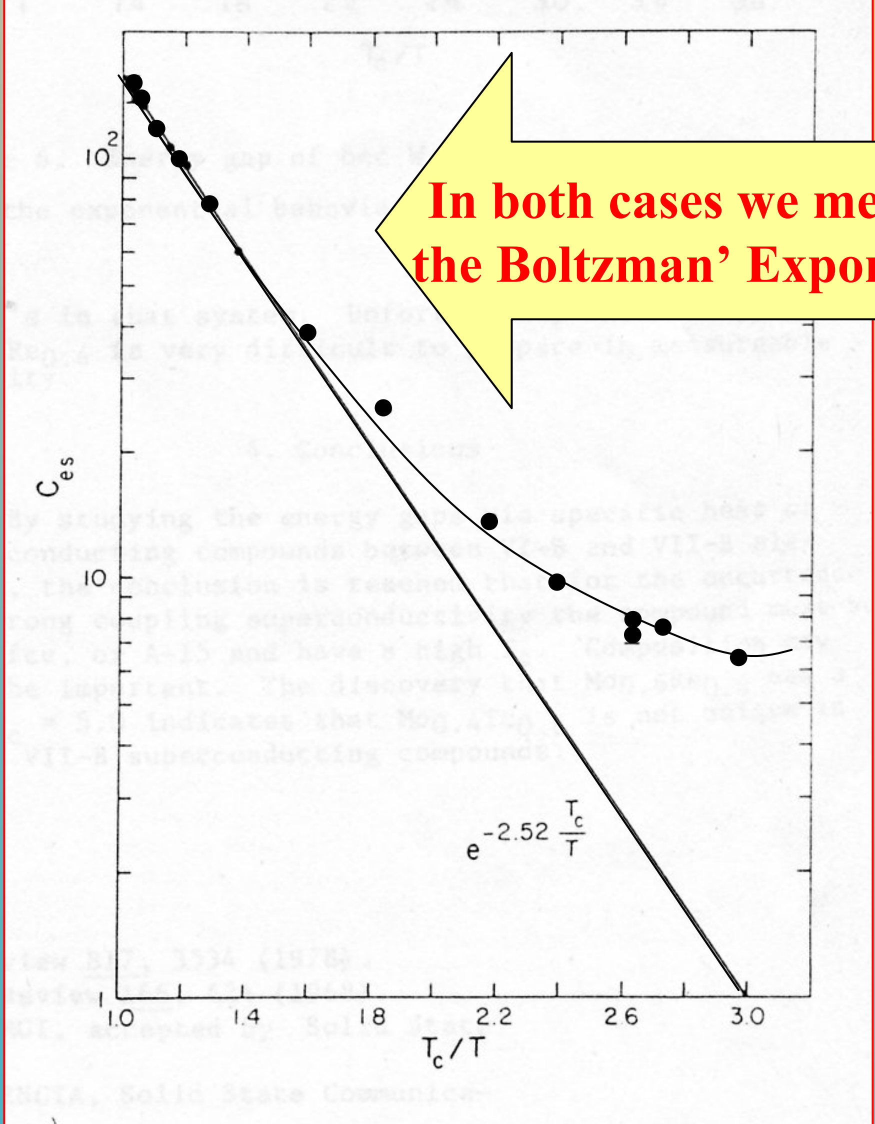

Figure 4. Energy gap of bcc $Mo_{0.6}Re_{0.4}$, derived from the exponential behaviour of C_{es} below T_c.